Cardiovascular Research

Zinc ameliorates human aortic valve calcification through GPR39 mediated ERK1/2 signaling pathway

--Manuscript Draft--

Manuscript Number:	CVR-2019-1285R2
Full Title:	Zinc ameliorates human aortic valve calcification through GPR39 mediated ERK1/2 signaling pathway
Short Title:	Novel role of zinc in aortic valve calcification
Article Type:	Original Article
Keywords:	Zinc, valve interstitial cell calcification, apoptosis, ERK1/2, GPR39
Corresponding Author:	Dongxing Zhu Guangzhou Medical University Guangzhou, Guangdong CHINA
Corresponding Author Secondary Information:	
Corresponding Author's Institution:	Guangzhou Medical University
Corresponding Author's Secondary Institution:	
First Author:	Ziying Chen
First Author Secondary Information:	
Order of Authors:	Ziying Chen
	Flora Gordillo-Martinez
	Lei Jiang
	Pengcheng He
	Wanzi Hong
	Xuebiao Wei
	Katherine A Staines
	Vicky E Macrae
	Chunxiang Zhang
	Danqing Yu
	Xiaodong Fu
	Dongxing Zhu
Order of Authors Secondary Information:	
Abstract:	Aims: Calcific aortic valve disease is the most common heart valve disease in the Western world. It has been reported that zinc is accumulated in calcified human aortic valves. However, whether zinc directly regulates calcific aortic valve disease is yet to be elucidated. The present study sought to determine the potential role of zinc in the pathogenesis of calcific aortic valve disease. Methods and Results: Using a combination of a human valve interstitial cell calcification model, human aortic valve tissues and blood samples, we report that 20 μM zinc supplementation attenuates human valve interstitial cell (hVIC) in vitro calcification, and that this is mediated through inhibition of apoptosis and osteogenic differentiation via the zinc sensing receptor GPR39-dependent ERK1/2 signaling pathway. Furthermore, we report that GPR39 protein expression is dramatically reduced in calcified human aortic valves, and there is a significant reduction in zinc serum levels in patients with calcific aortic valve disease. Moreover, we reveal that 20

	μM zinc treatment prevents the reduction of GPR39 observed in calcified human valve interstitial cells. We also show that the zinc transporter ZIP13 and ZIP14 are significantly increased in hVICs in response to zinc treatment. Knockdown of ZIP13 or ZIP14 significantly inhibited hVIC in vitro calcification and osteogenic differentiation. Conclusions: Together, these findings suggest that zinc is a novel inhibitor of calcific aortic valve disease, and report that zinc transporter ZIP13 and ZIP14 are important regulators of hVIC in vitro calcification and osteogenic differentiation. Zinc supplementation may offer a potential therapeutic strategy for calcific aortic valve disease. Translational Perspective This study reports that the zinc sensing receptor GPR39 expression is decreased in calcified human aortic valve tissues and there is a significant reduction in zinc serum levels in patients with calcific aortic valve disease. Zinc treatment attenuates hVIC in vitro calcification through inhibition of apoptosis and osteogenic differentiation via GPR39-dependent ERK1/2 signaling pathway. Zinc transporter ZIP13 and ZIP14 are important regulators of hVIC in vitro calcification and osteogenic differentiation. Zinc supplementation is a potential therapeutic strategy for calcific aortic valve disease.

Abstract

Aims: Calcific aortic valve disease is the most common heart valve disease in the Western world. It has been reported that zinc is accumulated in calcified human aortic valves. However, whether zinc directly regulates calcific aortic valve disease is yet to be elucidated. The present study sought to determine the potential role of zinc in the pathogenesis of calcific aortic valve disease.

Methods and Results: Using a combination of a human valve interstitial cell calcification model, human aortic valve tissues and blood samples, we report that 20 μM zinc supplementation attenuates human valve interstitial cell (hVIC) *in vitro* calcification, and that this is mediated through inhibition of apoptosis and osteogenic differentiation via the zinc sensing receptor GPR39-dependent ERK1/2 signaling pathway. Furthermore, we report that GPR39 protein expression is dramatically reduced in calcified human aortic valves, and there is a significant reduction in zinc serum levels in patients with calcific aortic valve disease. Moreover, we reveal that 20 μM zinc treatment prevents the reduction of GPR39 observed in calcified human valve interstitial cells. We also show that the zinc transporter ZIP13 and ZIP14 are significantly increased in hVICs in response to zinc treatment. Knockdown of ZIP13 or ZIP14 significantly inhibited hVIC *in vitro* calcification and osteogenic differentiation.

Conclusions: Together, these findings suggest that zinc is a novel inhibitor of calcific aortic valve disease, and report that zinc transporter ZIP13 and ZIP14 are important regulators of hVIC *in vitro* calcification and osteogenic differentiation. Zinc supplementation may offer a potential therapeutic strategy for calcific aortic valve disease.

Translational Perspective

This study reports that the zinc sensing receptor GPR39 expression is decreased in calcified human aortic valve tissues and there is a significant reduction in zinc serum levels in patients with calcific aortic valve disease. Zinc treatment attenuates hVIC *in vitro* calcification through inhibition of apoptosis and osteogenic differentiation via GPR39-dependent ERK1/2 signaling pathway. Zinc transporter ZIP13 and ZIP14 are important regulators of hVIC *in vitro* calcification and osteogenic differentiation. Zinc supplementation is a potential therapeutic strategy for calcific aortic valve disease.

Key words: Zinc, valve interstitial cell calcification, apoptosis, ERK1/2, GPR39

Guangzhou, 08.03.2020

Cardiovascular Research- CVR-2019-1285R2

Dear, Prof. Magnus Bäck

We are pleased to submit our revised manuscript 'Zinc ameliorates human aortic valve calcification through GPR39 mediated ERK1/2 signaling pathway' for your kind consideration. We confirm that this manuscript is not submitted elsewhere or under consideration for publication. All authors have read and agreed with the submission of the manuscript.

We thank the reviewers for their highly constructive comments and suggestions, and we have revised our manuscript accordingly. This has entailed editing and adding new text and data. New text is highlighted in red font. Below we have listed each of the reviewers' comments and provided our detailed response. We believe that our manuscript is much improved, and we hope that it is now considered suitable for publication in Cardiovascular Research.

Yours sincerely

On behalf of all authors

Dongxing Zhu, Ph.D

Associated Professor,

Guangzhou Institute of Cardiovascular Diseases, The Second Affiliated Hospital, Guangzhou Medical University,

Guangzhou 510260, Guangdong, China. Tel: +86. (0) 20.3710 3613. Email: dongxing.zhu@gzhmu.edu.cn

Cardiovascular Research- CVR-2019-1285R2

Authors' response to reviewers' comments

Reviewer #1:

Reviewer comment 1:

Just one minor thing I can't help but mention-in the revised discussion:

'Our data suggest that knockdown of ZIP13 or ZIP14 may reduce hVIC calcification through attenuation of osteogenic transition. In addition, ALP, a key regulator of cardiovascular calcification, have been reported to contain two zinc-binding sites, which are essential for its catalytic activity37. We have shown that knockdown of ZIP13 or ZIP14 decreased cytosolic zinc concentrations, which may lead to reduced catalytic activity of ALPL, thereby inhibiting calcification.'

I find this statement highly speculative and not very straightforward as a mechanism. ALP could be expected to be mediating pro-calcific effects in the extracellular space, if the reduction of intracellular zinc would impair enzyme function is rather far stretched. My recommendation would be to omit that and to state "The mechanisms underlying the anti-calcific effects of ZIP13 or ZIP14 silencing are currently elusive and require further study." Or similar, if the authors choose to do so.

Authors' response: We thank the reviewer's comments and suggestions. We have revised our text accordingly.

Discussion: Line 504-506

'The mechanisms underlying the anti-calcific effects of ZIP13 or ZIP14 silencing are currently elusive and require further study.'

Reviewer #3:

Reviewer comment 1: Please provide echo data for patients in Suppl. Table II.

Authors' response: We are extremely sorry that we did not record the echo data for patients in Suppl. Table II at the time of sample collection. In the present study, alizarin red staining was used to measure calcium deposition in these aortic valve samples. As shown in Figure 6A, positive staining of alizarin red was observed in calcified aortic valves, while no staining of alizarin red was seen in non-calcified aortic valves.

Reviewer comment 2: In Suppl. Table III, according to the legend ARA would be «aortic

regurgitation area» in cm2; the meaning is not clear. If AR was significant, it should be documented by the regurgitant fraction and ERO. Please clarify as if these patients had significant AR including these data makes probably no sense. It appears that this group of patients had aortic valve sclerosis, it should be underlined in the result section.

Authors' response: We thank the reviewers' comments. In china, aortic regurgitation area is the routinely used index in clinical practice to evaluate the severity of AR, and the regurgitant fraction and ERO are not routinely measured by echo in the hospitals in china. We are sorry that we cannot collect these two specific variables. We agree with the reviewer's comments, and we have removed ARA «aortic regurgitation area» from Suppl. Table III in our revised manuscript. We agree with the reviewer's comments that this group of patients had aortic valve sclerosis, and we have highlighted it in the results section as below.

Results: Line 413-416

'These patients had aortic valve sclerosis, which is an early stage of CAVD and characterized by thickening and calcification of the aortic valve without obstruction of ventricular outflow (Supplementary Figure I and Supplementary material Table III).'

Reviewer comment 3: Fluorescent assay and IF in figure 5H (for Zn) and 7A need to be quantified.

Authors' response: We have quantified Fluorescent assay and IF in figure 5H (for Zn) and 7A in our revised manuscript. These new data are presented as Figure 5I and revised Figure 7A (lower panel).

Zinc ameliorates human aortic valve calcification through GPR39 mediated ERK1/2 signaling pathway

Ziying Chen[1#], Flora Gordillo-Martinez[1#], Lei Jiang[2#], Pengcheng He[3], Wanzi Hong[3], Xuebiao Wei[3], Katherine A Staines[4], Vicky E. Macrae[5], Chunxiang Zhang[6], Danqing Yu[3*], Xiaodong Fu[1*], Dongxing Zhu[1*]

1. Guangzhou Institute of Cardiovascular Disease, Guangdong Key Laboratory of Vascular Diseases, State Key Laboratory of Respiratory Disease, the Second Affiliated Hospital, Guangzhou Medical University, Guangzhou, Guangdong, 510260, P.R.China.
2. Guangdong Geriatric Institute, Guangdong Provincial People's Hospital, Guangdong Academy of Medical Sciences, Guangzhou 510080, China.
3. Department of Cardiology, Guangdong Cardiovascular Institute, Guangdong Provincial Key Laboratory of Coronary Heart Disease Prevention, Guangdong Provincial People's Hospital, Guangdong Academy of Medical Sciences, Guangzhou 510100, China.
4. School of Applied Sciences, Edinburgh Napier University, Edinburgh, EH11 4BN, UK.
5. The Roslin Institute, RDSVS, Easter Bush Campus, University of Edinburgh, Midlothian, EH25 9RG, UK.
6. Department of Biomedical Engineering, School of Medicine, The University of Alabama at Birmingham, Birmingham, AL 35233, USA.

Short title: Novel role of zinc in aortic valve calcification

[#]These authors contributed equally to this work.

[*]**Address for correspondence:** Dongxing Zhu, PhD, Guangzhou Institute of Cardiovascular Disease, Guangdong Key Laboratory of Vascular Diseases, State Key Laboratory of Respiratory Disease, the Second Affiliated Hospital, Guangzhou Medical University, Guangzhou, Guangdong, 510260, P.R.China. Email: dongxing.zhu@gzhmu.edu.cn, Tel: +86.020.37103613; Xiaodong Fu, PhD, Guangzhou Institute of Cardiovascular Disease, Guangdong Key Laboratory of Vascular Diseases, State Key Laboratory of Respiratory Disease, the Second Affiliated Hospital, Guangzhou Medical University, Guangzhou, Guangdong, 510260, P.R.China. Email: fuxiaod@gzhmu.edu.cn, Tel: +86.020.83412002; Danqing Yu, MD, PhD, Department of Cardiology, Guangdong Cardiovascular Institute, Guangdong General Hospital, Guangdong Academy of Medical Sciences, Guangzhou 510080, China. Email: gdydq100@126.com, Tel: +86.020.83827812.

The category of the manuscript: Original Article

Word count: 9617

List of Abbreviations

CAVD- Calcific aortic valve disease, LVEF- Left ventricular ejection fraction, RUNX2- Runt-related transcription factor 2, VICs- Valve interstitial cells, TGFβ1- Transforming growth factor -β1, TRAIL- TNF-related apoptosis-inducing ligand, NF-κB- Nuclear factor κB, VSMCs- Vascular smooth muscle cells, GPR39- G protein coupled receptor 39, TNFAIP3- TNF-α–induced protein 3, TPEN- N,N,N',N'-tetrakis (2-pyridinylmethyl)-1,2-ethanediamine, BCA- Bicinchoninic acid, PMSF- Phenylmethylsulfonyl fluoride, ALPL- Alkaline phosphatase, MSX2- Msh Homeobox 2, BMP- Bone morphogenetic protein, CKD- Chronic kidney disease.

Abstract

Aims: Calcific aortic valve disease is the most common heart valve disease in the Western world. It has been reported that zinc is accumulated in calcified human aortic valves. However, whether zinc directly regulates calcific aortic valve disease is yet to be elucidated. The present study sought to determine the potential role of zinc in the pathogenesis of calcific aortic valve disease.

Methods and Results: Using a combination of a human valve interstitial cell calcification model, human aortic valve tissues and blood samples, we report that 20 μM zinc supplementation attenuates human valve interstitial cell (hVIC) *in vitro* calcification, and that this is mediated through inhibition of apoptosis and osteogenic differentiation via the zinc sensing receptor GPR39-dependent ERK1/2 signaling pathway. Furthermore, we report that GPR39 protein expression is dramatically reduced in calcified human aortic valves, and there is a significant reduction in zinc serum levels in patients with calcific aortic valve disease. Moreover, we reveal that 20 μM zinc treatment prevents the reduction of GPR39 observed in calcified human valve interstitial cells. We also show that the zinc transporter ZIP13 and ZIP14 are significantly increased in hVICs in response to zinc treatment. Knockdown of ZIP13 or ZIP14 significantly inhibited hVIC *in vitro* calcification and osteogenic differentiation.

Conclusions: Together, these findings suggest that zinc is a novel inhibitor of calcific aortic valve disease, and report that zinc transporter ZIP13 and ZIP14 are important regulators of hVIC *in vitro* calcification and osteogenic differentiation. Zinc supplementation may offer a potential therapeutic strategy for calcific aortic valve disease.

Translational Perspective

This study reports that the zinc sensing receptor GPR39 expression is decreased in calcified human aortic valve tissues and there is a significant reduction in zinc serum levels in patients with calcific aortic valve disease. Zinc treatment attenuates hVIC *in vitro* calcification through inhibition of apoptosis and osteogenic differentiation via GPR39-dependent ERK1/2 signaling pathway. Zinc transporter ZIP13 and ZIP14 are important regulators of hVIC *in vitro* calcification and osteogenic differentiation. Zinc supplementation is a potential therapeutic strategy for calcific aortic valve disease.

Key words: Zinc, valve interstitial cell calcification, apoptosis, ERK1/2, GPR39

1. Introduction

Calcific aortic valve disease (CAVD), the most common heart valve disease, is a major public health problem in the Western world. It is a chronic disorder that is characterized by progressive fibrocalcific valve thickening and ventricular function impairment, subsequently leading to left ventricular outflow obstruction[1]. Traditional cardiovascular drugs such as statins are unable to prevent the progression of CAVD. Currently, the viable treatments for patients with severe CAVD are surgical valve replacement or transcatheter aortic valve implantation with the prosthetic valves[2]. However, these treatments are invasive, costly and risky for elderly adults, and it may lead to more severe complications including blood clots, infections, and heart attack. In addition, the prosthetic valves have limited durability, and undergo structural degeneration and calcification[3]. A better understanding of the pathophysiology of CAVD is therefore critical for the development of novel therapeutic strategies to slow or reverse the progression of CAVD.

Accumulating evidence indicates that CAVD is an actively regulated and progressive disease, which shares many similarities to physiological bone mineralization. Osteogenic genes like runt-related transcription factor 2 (RUNX2) have been shown to be up-regulated in calcified human aortic valves[4]. Patients with chronic kidney disease (CKD) have increased circulating calcium (Ca) and phosphate (Pi) levels, and are highly susceptible to CAVD[5, 6]. Accordingly, we and others have previously reported that valve interstitial cells (VICs), the most abundant cell type in the aortic valve, undergo osteogenic differentiation in response to high Ca and Pi mimicking that observed in CKD patients[7, 8]. Based on these observations, it is now recognized that the osteogenic differentiation of VICs plays an important role in the development of CAVD. Furthermore, cytokines involved in calcification including the transforming growth factor-β1 (TGFβ1) and TNF-related apoptosis-inducing ligand (TRAIL) are overexpressed in calcific aortic valves[9, 10]. These cytokines promote aortic valve calcification through induction of VIC apoptosis[9, 10]. Conversely, pro-survival signals like ATP have been shown to prevent aortic valve calcification[11]. These studies suggest that apoptosis is also involved in the pathogenesis of CAVD.

Zinc is an important micronutrient for health, which modulates numerous cellular processes including DNA and protein synthesis, enzyme activity, and intracellular signaling. Zinc deficiency is associated with cardiovascular disease. It has been shown that zinc deficiency enhances vascular inflammation and atherosclerotic plaque formation in ApoE knockout mice[12]. Accordingly, zinc supplementation attenuates a high cholesterol diet-induced atherosclerosis in rabbits[13]. Zinc has also been reported to inhibit abdominal aortic aneurysm formation in mice through induction of zinc finger protein A20-mediated suppression of nuclear factor κB (NF-κB) pathway[14]. Furthermore, a recent study has demonstrated that zinc ameliorates phosphate-induced osteogenic transition of vascular smooth muscle cells (VSMCs) and vascular calcification through the G protein coupled receptor 39 (GPR39)-dependent induction of TNF-α–induced protein 3 (TNFAIP3) and subsequent suppression of the NF-kB pathway[15]. Interestingly, zinc has been shown to be accumulated in calcified human aortic valves[16]. However, the role of zinc in the development

of CAVD has not been previously investigated.

In the present study, we have performed detailed analysis of clinical samples from patients with CAVD in conjunction with *in vitro* calcification studies in hVICs to address the possible effects of zinc and zinc transporters on aortic valve calcification and the underlying mechanisms through which zinc and zinc transporters may regulate CAVD.

2. Experimental procedures

2.1 Human samples

This study complies with the Declaration of Helsinki and approved by The Research Ethics Committee of Guangdong Provincial People's Hospital and Guangzhou Medical University (Ref No: GDREC2019433H). 34 tricuspid aortic valves from patients with CAVD (25 males/9 females) and 4 non-calcified aortic valves from patients with aortic valve prolapse (4 males) undergoing valve replacement surgery were collected at Guangdong Provincial People's Hospital (Guangzhou, China). Marked increase in echogenicity of aortic valves measured by echocardiograms was considered as CAVD by clinical doctors. A representative still image of echocardiograms of a patient with CAVD is shown in Supplementary Figure I. Patients with a history of rheumatic disease, congenital valve disease, and infective endocarditis were excluded. Human blood samples were also collected from 15 healthy volunteers and 15 patients with CAVD at Guangdong Provincial People's Hospital (Guangzhou, China). Informed consent was obtained from all patients. Serum was obtained by immediate centrifugation and stored at -80°C. Clinical characteristics of the patients used in the present study are summarized in Supplementary material Table I-III. The methodology, conduct, and reporting of this study were in accordance with the Strengthening the Reporting of Observational Studies in Epidemiology (STROBE) Statement initiatives for case-control studies[17]. STROBE recommendations for reporting case-control studies are available as Supplementary material Table IV.

2.2 Measurement of zinc serum levels

Zinc concentrations were analyzed by an automatic biochemical analyzer (Chemray 240) with the Zinc Assay Kit (Changchun Huili Biotech, C017) according to the manufacturer's instructions.

2.3 Isolation of Human Valve Interstitial Cells (hVICs)

hVICs were isolated from non-calcified areas of the valves from patients with CAVD, and the purity of cell preparation was characterized as previously described[8]. Briefly, non-calcified areas of valve leaflets were dissected, incubated with 1 mg/ml trypsin (Gibco, 12605-010) for 10 min and washed in HBSS buffer (Hyclone, SC30588.01) to remove valve endothelial cells. The valve tissues were then digested in 250 U/ml type II collagenase solution (Worthington, 47D17411A) at 37°C for 7 hrs. The cells subsequently obtained were re-suspended in growth media consisting of α-MEM supplemented with 10% FBS (Gibco, 16000-044), 100 U/mL of penicillin (HyClone, SH40003.01), and 100 mg/ml of streptomycin (Hyclone, SV30010), and plated onto a 25 cm^2 flask coated with 0.25 $\mu g/cm^2$ type I collagen

(Gibco, A1048301). Cells used for experiments in the present study were between 2-4 passages.

2.4 Induction of hVIC *in vitro* calcification

hVICs were seeded at the density of $1.0x10^5$ cells/well in 6-well plates and cultured with growth media. Calcification was induced as previously described[8]. Briefly, hVICs were grown to confluence and treated with control (1.0 mM Pi/1.8mM Ca) or calcifying media (50 μg/mL ascorbic acid/2.5 mM Pi/2.7 mM Ca) for up to 7 days. Pi was prepared as a combination of NaH_2PO_4/Na_2HPO_4, pH=7.4. To evaluate the effects of zinc on hVIC *in vitro* calcification, the indicated concentrations (0-20 μM) of $ZnSO_4$ (Sigma, Z2051), the specific zinc chelator N,N,N',N'-tetrakis (2-pyridinylmethyl)-1,2-ethanediamine (TPEN) (Sigma, P4431), $ZnCl_2$ (Sigma, 746355), albumin (Sigma, SRP6516) and ERK1/2 inhibitor PD98059 (Cell Signaling Technology, 9900) were added to the culture media. The media was changed every third/fourth day.

2.5 Determination of hVIC *in vitro* calcification

Calcium deposition was determined by alizarin red staining and calcium colorimetric assay. Briefly, the cells were washed twice with cold PBS, fixed with 4% paraformaldehyde (PFA) for 10 min, stained with 2% alizarin red (pH 4.2) for 10 min at room temperature, and photographed. The cells were also decalcified with 0.6 M HCl at 4ºC overnight. Free calcium in the supernatants was determined using a calcium colorimetric assay (Sigma, MAK022-1KT) according to the manufacturer's instructions. Cells were washed with PBS twice and harvested in lysis buffer (1 mM NaOH/0.1% SDS) for protein extraction. The total protein concentration was determined with bicinchoninic acid (BCA) protein assay kit (Thermo Fisher, 23235). Calcium content was normalized to total cell protein and expressed as μg/mg protein.

2.6 Intracellular zinc detection

hVICs were cultured with control or calcifying media in the presence of 20 μM $ZnSO_4$ and/or 20μM TPEN for up to 7 days. Intracellular zinc was detected using the zinc-selective indicator FluoZin-3 AM (Invitrogen, F24195) following the manufacturer's instructions. Briefly, cells were incubated with 1 μM of FluoZin-3 AM containing 0.02% Pluronic F-127 (Invitrogen, F24195) for 30 min at 37ºC. After washing with Ca^{2+} and Mg^{2+} free PBS, cells were incubated for an additional 30 min at 37ºC, and mounted in warm PBS buffer containing DAPI. Fluorescence images were detected by excitation at 488 nm and emission at 542 nm under a Leica DMRB fluorescence microscope (Leica SP8).

2.7 Immunofluorescence staining

To evaluate the expression of GPR39, hVICs were cultured with control or calcifying media in the presence or absence of 20 μM $ZnSO_4$ for up to 7 days. Cells were fixed, permeabilized with 0.3% triton x-100 (Beyotime Biotechnology, P0013B) and incubated overnight at 4°C with anti-GPR39 (1:500, Abcam, ab229648). After washing with PBS, cells were incubated with Alexa Fluor®488 anti-rabbit antibodies (1:1000, Invitrogen, A11008) in blocking buffer at 37 °C for 1 hr in the dark. Glass coverslips were then stained with DAPI

and fluorescence signal was detected under Leica DMRB fluorescence microscope (Leica SP8). Negative controls were carried out simultaneously by incubating with equivalent concentrations of normal rabbit IgG (Santa Cruz, sc2025) instead of primary antibody.

2.8 Quantitative RT-PCR

Total RNA was extracted from hVICs using TaKaRa MiniBEST Universal RNA Extraction Kit (Takara, 9767) and from human aortic valves using Trizol (Invitrogen, 1596026) according to the manufacturers' instructions. RNA was quantified and reverse transcribed using PrimeScript™ RT Master Mix (Takara, RR036A). Quantitative RT-PCR was performed with SYBR Premix Ex Taq II (Takara, RR820A) in the QuantStudio 5 real-time system (Life technologies). Each PCR was run in triplicate. All gene expression data were calculated using the $2^{-\Delta\Delta CT}$ method and normalized against GAPDH. The control values were expressed as 1 to indicate a precise fold change value for each gene of interest. The primer sequences for target genes are summarized in Supplementary material Table V.

2.9 Transfection of siRNAs

hVICs were seeded at the density of 1.0×10^5 cells/well in 6-well plates and transfected with 25 nM *GPR39* siRNA (RIBOBIO), *ZIP13* siRNA (RIBOBIO), *ZIP14* siRNA (RIBOBIO), *ERK1/2* siRNA (RIBOBIO) or Non-targeting (siNC) siRNA (RIBOBIO) using Lipofectamine RNAiMAX (Invitrogen, 13778) following the manufacturer's instructions. The knockdown efficiency of siRNAs used in the present study was confirmed by quantitative RT-PCR and western blotting. For long-term hVIC *in vitro* calcification, cells were re-transfected at day 3 and incubated with calcifying media for up to 7 days. The siRNA sequences for gene silencing are summarized in Supplementary material Table VI.

2.10 Western blotting

hVICs were harvested with RIPA lysis buffer (Beyotime Biotechnology, P0013B) containing 1 mM protease inhibitor phenylmethylsulfonyl fluoride (PMSF) (Beyotime Biotechnology, ST505). Western blotting was performed. Equal amounts of protein lysates were separated on SDS-Polyacrylamide gels and transferred to PVDF membranes. The membranes were incubated overnight at 4 °C with primary antibodies: anti-caspase 3 (1:2000, Cell Signaling Technology, 9662S), anti-cleaved caspase 3 (1:2000, Cell Signaling Technology, 9664S), anti-pAKT (1:4000, Cell Signaling, 4060S), anti-AKT (1:4000, Cell Signaling Technology, 9272), anti-pERK (1:4000, Cell Signaling Technology, 9101), anti-ERK (1:4000, Cell Signaling Technology, 4695), Anti-GPR39 (1:2000, Abcam, ab229648), Anti-RUNX2 (1:2000, Abcam, ab23981), Anti-MSX2 (1:2000, Santa Cruz, sc-393986), Anti-ZIP13 (1:2000, Abcam, ab106586), Anti-ZIP14 (1:2000, Abcam, ab106568), anti-β-actin (1:2000, Santa Cruz, J1116). Subsequently, membranes were incubated with HRP-conjugated anti-mouse (1:4000, Cell Signaling Technology, 7076S) or anti-rabbit (1:4000, Cell Signaling Technology, 7074S) secondary antibodies for 1 hr at room temperature. The immune complexes were visualized by chemiluminescence Lumi-Light Western Blotting Substrate (Millipore, WBKLS0500). Semi-quantitative assessment of band intensity was achieved by using ImageJ software (National Institutes of Health).

221 **2.11 Cell death assay**

222 hVICs were seeded at a density of $1.0x10^4$/wells in 96-well plates and incubated with
223 control or calcifying media in the presence or absence of 20 μM $ZnSO_4$ for up to 7 days. Cell
224 death was measured using Cytotoxicity lactic dehydrogenase (LDH) Assay Kit (Beyotime
225 Biotechnology, C0038) following the manufacturer's instructions.
226

227 **2.12 Calcium phosphate precipitation assay**

228 Calcium phosphate precipitation assay was performed as previously described[15]. Briefly,
229 the indicated concentrations of $ZnSO_4$ (0-20μM) was incubated with a homogeneous system
230 containing 10 mM $CaCl_2$ (Sigma, 793639) and 10 mM sodium phosphate buffer (pH7.4,
231 Sigma, 342483) in 500 mM HEPES buffer (pH7.4, Sigma, RDD002) for 10 min at room
232 temperature. The samples were then centrifuged at 1890g for 30 sec and the obtained pellet
233 was dissolved in 0.6 M HCl. Calcium content in the pellet was determined using a calcium
234 colorimetric assay (Sigma, MAK022-1KT).
235

236 **2.13 Apoptosis assay**

237 Apoptotic hVICs were determined by manually counting pyknotic nuclei after staining
238 with DAPI (Cell Signaling, 4083S). In addition, hVICs in different stages of apoptosis were
239 analyzed by flow cytometry using Dead Cell Apoptosis Kit with Annexin V Alexa Fluor™
240 488 & Propidium Iodide (PI) (Invitrogen, V13241) according to the manufacturer's
241 instructions. In brief, hVICs were cultured with control or calcifying media in the presence or
242 absence of 20 μM $ZnSO_4$ for 3 days. Cells were harvested by trypsinization, washed with cold
243 PBS and stained with Annexin V Alexa Fluor™ 488 and PI. 30,000 cell events were recorded
244 on a BD FACS Calibur (Becton, Dickinson & Company) and data were analyzed with FlowJo
245 8.8.4 flow cytometry analysis software (Tree Star Inc.).
246

247 **2.14 Histology and immunohistochemistry**

248 Human aortic valves tissues were fixed with 4% PFA for 24 hrs, dehydrated and
249 embedded in paraffin wax before sectioning at 7 μm using standard procedures. For
250 evaluation of calcium deposition, sections were de-waxed in xylene and stained with 2%
251 Alizarin Red S solution for 5 min. After removal of the excess dye, sections were rinsed in
252 100% acetone and %50:%50 acetone-xylene. Sections were then cleared in 100% xylene for 5
253 min and mounted using neutral balsam (Solarbio, G8590). Light microscopy images were
254 obtained by a scanning light microscope (Leica CS2).
255

256 For immunohistochemistry, sections were subjected to sodium citrate (pH 6.0) for
257 antigen retrieval for 10 min at 95 °C. Endogenous peroxidase activity and non-specific
258 antibody binding were blocked before overnight incubation at 4 °C with anti-GPR39 antibody
259 (1:500, Abcam, ab229648). The sections were then washed in PBS, and incubated with
260 secondary antibody using ChemMate™ EnVision™ Detection Kit (Gene Tech, GK500710)
261 following the manufacturer's instructions. The sections were finally counterstained with
262 haematoxylin and eosin, dehydrated, and mounted in neutral balsam (Solarbio, G8590).
263 Control sections were incubated with equal concentrations of normal rabbit IgG (Santa Cruz,
264 sc2025) in place of the primary antibody. Images were obtained with a digital whole slide

scanner (Leica Aperio CS2).

2.15 Statistical analysis

All experiments were repeated at least 3 times and the representative results are shown. All values are expressed as mean ±SEM. Statistical analysis was performed using GraphPad Prism 6 (La Jolla, CA) software. After confirming a normal distribution using the Shapiro-Wilk test, data were analysed using unpaired Student's t-test for comparison of two groups, one-way analysis of variance followed by Bonferroni post-test for comparison of multiple groups or a suitable non-parametric test such as Mann–Whitney. $P< 0.05$ was considered to be statistically significant.

3. Results

3.1 Zinc supplementation inhibits hVIC *in vitro* calcification and osteogenic differentiation

Initial studies were performed to validate the hVIC *in vitro* calcification model. In accordance with our previous report[8], hVICs showed positive staining for both SM22-α and Vimentin (Supplementary Figure II A). As revealed by alizarin red staining and quantitative calcium analysis, hVICs cultured under calcifying media showed significantly increased calcium deposition (12.15 fold, $p<0.001$; Supplementary Figure II B and C) at day 7. The osteogenic related genes including alkaline phosphatase (*ALPL*) (3.8 fold, $p<0.001$), Msh Homeobox 2 (*MSX2*) (3.9 fold, $p<0.01$), and *RUNX2* (1.6 fold, $p<0.001$) were dramatically up-regulated in calcified hVICs compared to non-calcified hVICs (Supplementary Figure II D). Furthermore, increased cell death (11.5% at Day7, $p<0.001$) and apoptosis (2.0 fold, $p<0.05$) were observed during the process of hVIC *in vitro* calcification (Supplementary Figure II E and F). These results are consistent with previous reports[4, 8].

To evaluate the possible effects of zinc on hVIC *in vitro* calcification, hVICs were treated with 5-20 μM $ZnSO_4$ in the presence of calcifying media for up to 7 days. Alizarin red staining and quantitative calcium analysis showed that 20μM $ZnSO_4$ significantly attenuated calcium deposition in hVICs at day 7 (53% decrease, $p<0.001$; Figure 1A and 1B). To determine whether the inhibitory effect of $ZnSO_4$ on hVICs *in vitro* calcification was specifically due to zinc ions, a specific zinc chelator TPEN was used. FluoZin-3 (a zinc-selective indicator) staining revealed that 20 μM TPEN dramatically abolished zinc accumulation in hVICs treated with 20 μM $ZnSO_4$ at day 3 and day 7 (Figure 1C). As expected, 20 μM TPEN significantly blunted the inhibitory effect of 20 μM $ZnSO_4$ on hVIC *in vitro* calcification ($p<0.001$; Figure 1D). Furthermore, $ZnCl_2$ treatment also significantly inhibited calcium deposition in hVICs at day 7 (39% decrease, $p<0.001$; Figure 1E). Considering the important role of osteogenic differentiation of hVICs in aortic valve calcification[4, 8], we next assessed whether zinc supplementation could reduce osteogenic related gene expression in hVICs. The up-regulation of *ALPL* and *MSX2* in hVICs induced by calcifying media was significantly attenuated by zinc treatment after 7 days (Figure 1F and 1G). It has been reported that serum albumin is the major zinc carrier in blood and responsible for its system distribution[18]. We showed that 1mg/ml albumin did not alter the inhibitory

effect of zinc on hVIC calcification (Figure 1H). Taken together, these data suggest that zinc supplementation specifically inhibits hVIC *in vitro* calcification.

3.2 Zinc prevents apoptosis during hVIC *in vitro* calcification

Apoptosis has been previously reported to play a crucial role in initiation and progression of aortic valve calcification[9-11], we therefore undertook a detailed assessment of apoptosis in hVICs following zinc treatment. 20 μM $ZnSO_4$ treatment significantly reduced cell death ($p<0.05$; Figure 2A), apoptotic nuclei ($p<0.001$; Figure 2B) and apoptosis (50% decrease, $p<0.05$; Figure 2C) in hVICs cultured with calcifying media. Western blotting also showed that zinc supplementation prevented up-regulation of cleaved caspase3 in hVICs cultured with calcifying media at day 7 (Figure 2D, $p<0.05$). Calcium phosphate precipitation was not affected by $ZnSO_4$ treatment (Figure 2E). In addition, zinc supplementation did not alter calcium phosphate deposition on fixed hVICs (Supplementary Figure III A and B). These data suggest no direct physicochemical inhibition of calcium/phosphate deposition by $ZnSO_4$. We further examined the expression of TNFα and TFGβ, which are the important cytokines that involved in calcification through regulation of apoptosis[9, 10]. Zinc supplementation significantly attenuated the up-regulation of *TNFα* mRNA expression during hVIC *in vitro* calcification (45.2% decrease, Figure 2F, $p<0.01$). However, *TGFβ* mRNA expression was not altered in hVICs cultured with calcifying media in the absence or presence of zinc supplementation (Figure 2G). Taken together, our data suggests that zinc supplementation reduces hVIC *in vitro* calcification at least in part through inhibition of apoptosis.

3.3 Zinc inhibits hVIC *in vitro* calcification and apoptosis through activation of the ERK1/2 signaling pathway

To elucidate the underlying mechanisms of the protective effect of zinc on hVIC calcification, we investigated the activation of AKT and EKR1/2, which have been previously reported as key regulators of hVIC calcification[19, 20]. 20 μM $ZnSO_4$ treatment significantly induced phosphorylation of ERK1/2 after 10 min ($p<0.01$) and 30 min ($p<0.01$), but not after 60 min, while AKT phosphorylation was not induced by addition of $ZnSO_4$ (Figure 3A). 20 μM $ZnSO_4$ treatment effectively inhibited hVIC *in vitro* calcification, as determined by alizarin red staining (Figure 3B) and calcium quantitative analysis ($p<0.001$, Figure 3C). Accordingly, the inhibitory effect of $ZnSO_4$ on hVIC calcification was significantly abolished in the presence of the ERK1/2 inhibitor PD98059 ($p<0.01$, Figure 3B and 3C). ERK1/2 inhibitor PD98059 by itself had no effect on hVIC calcification (Supplementary Figure IV A and B). Moreover, the inhibition of $ZnSO_4$ on cleaved caspase3 (as an indication of apoptosis) expression ($p<0.01$, Figure 3D) and cell death ($p<0.01$, Figure 3E) in hVICs was also prevented by PD98059. In addition, siRNA-mediated knockdown of ERK1/2 also blunted the inhibitory effect of zinc on hVIC *in vitro* calcification ($p<0.05$, Figure 3F). ERK1/2 siRNA knockdown efficiency was confirmed by quantitative RT-PCR and western blotting (Supplementary Figure V A-C). These data support that activation of the ERK1/2 signaling pathway plays a key role in mediating the protective effect of zinc on hVIC calcification and apoptosis.

3.4 Zinc signals through the GPR39 receptor to activate ERK1/2 signaling pathway and

inhibit hVIC calcification

The zinc-sensing receptor GPR39 plays a key role in mediating zinc intracellular signaling pathways[21]. Additional experiments were therefore performed to examine the role of GPR39 in zinc mediated inhibition of hVIC calcification. The expression of GPR39 was detected in hVICs isolated from 5 patients with CAVD (Figure 4A). The endogenous expression of GPR39 was suppressed by transfection of GPR39 siRNA. Western blotting analysis showed that GPR39 siRNA 2 resulted in a significant reduction of GPR39 protein expression (Figure 4B). As expected, silencing of GPR39 attenuated zinc induced phosphorylation of ERK1/2 (20% decrease, $p<0.01$; Figure 4C). In addition, silencing of GPR39 by itself did not alter hVIC *in vitro* calcification, but significantly blunted the inhibitory effect of zinc supplementation on hVIC *in vitro* calcification ($p<0.05$; Figure 4D and E). siRNA knockdown of GPR39 also attenuated the inhibitory effects of zinc on hVIC apoptosis ($p<0.05$; Figure 4F) and the osteogenic gene *MSX2* ($p<0.05$; Figure 4G) and *BMP2* mRNA expression ($p<0.001$; Figure 4H). The inhibitory effect of zinc on *RUNX2* mRNA expression was not significantly affected by knockdown of GPR39 (Figure 4I). Our data support a key role of GPR39 in mediating the anti-calcific effects of zinc supplementation on hVICs.

3.5 Knockdown of *ZIP13* or *ZIP14* inhibits hVIC *in vitro* calcification

The human zinc transporter ZIP family consisting of 14 members functions to increase the cytosolic zinc accumulation by transporting zinc into the cytosol from the extracellular space or from intracellular compartments[22]. Among the 14 members of ZIP family examined, only *ZIP13* (5.0 fold, $p<0.05$) and *ZIP14* (1.8 fold, $p<0.05$) mRNA expression were significantly induced in hVICs treated with 20 μM $ZnSO_4$ (Figure 5A). We therefore undertook further analysis to investigate the functional role of *ZIP13* and *ZIP14* in hVIC calcification. Knockdown efficiency of *ZIP13* and *ZIP14* was confirmed by quantitative RT-PCR and western blotting (Supplementary Figure V D-I). Knockdown of *ZIP13* resulted in a significant decrease of calcium deposition in hVICs (30% decrease, $p<0.05$, Figure 5B and 5C). This inhibitory effect was further exacerbated in the presence of 20 μM $ZnSO_4$ (50% decrease, $p<0.05$, Figure 5B and 5C). Consistent with these data, knockdown of *ZIP13* significantly reduced mRNA expression of the osteogenic related gene *MSX2* (51.1% decrease, $p<0.001$, Figure 5F) in hVICs cultured with calcifying media after 7 days. However, this inhibition was abolished by zinc supplementation (Figure 5F). Knockdown of *ZIP13* also decreased the osteogenic gene *ALPL* mRNA expression in hVICs cultured with calcifying media in the absence (63.6% decrease, $p<0.05$, Figure 5G) or presence (70.8% decrease, $p<0.05$, Figure 5G) of 20 μM $ZnSO_4$ after 7 days. Knockdown of *ZIP14* attenuated hVIC *in vitro* calcification (19% decrease, $p<0.05$, Figure 5D and 5E), but the addition of zinc to the knockdown of ZIP14 did not provide further reduction of the calcification process in hVIC cultures (Figure 5E). In addition, knockdown of *ZIP14* resulted in a significant reduction in *MSX2* mRNA expression in hVICs cultured with calcifying media in the absence (51.1% decrease, $p<0.001$, Figure 5F) or presence (43.5% decrease, $p<0.01$, Figure 5F) of 20 μM $ZnSO_4$ after 7 days. However, knockdown of *ZIP14* did not alter *ALPL* mRNA expression in hVICs (Figure 5G). We did not see any significant difference in the expression of ZIP13 and ZIP14 between un-calcified and calcified human aortic valves (Supplementary Figure VI A

397 and B). Additionally, we observed that either knockdown of ZIP13 or ZIP14 dramatically
398 reduced the cytosolic zinc concentrations in hVICs in the absence or presence of zinc
399 supplementation (Figure 5H and 5I). Taken together, our data suggest an important role of
400 zinc transporter *ZIP13* and *ZIP14* in hVIC calcification and osteogenic differentiation.
401
402 **3.6 GPR39 expression is decreased in calcified human aortic valves**
403 To better understand the role of GPR39 in CAVD, expression of GPR39 was assessed in
404 4 non-calcified and 4 calcified human aortic valves. Clinical characteristics of these patients
405 are shown in Supplementary material Table II. Calcium deposition in human aortic valves was
406 confirmed by positive staining of alizarin red (Figure 6A). Immunohistochemistry showed
407 that GPR39 expression was dramatically decreased in calcified aortic valves compared to
408 non-calcified aortic valves (Figure 6A). This observation was further confirmed by a western
409 blotting analysis of 4 non-calcified aortic valves and 4 calcified aortic valves, which showed a
410 significant reduction of GPR39 expression in calcified human aortic valves (30% decrease,
411 $p<0.05$; Figure 6B). These data are the first to show that GPR39 expression is decreased in
412 calcified human aortic valves. Furthermore, zinc serum levels were also significantly
413 decreased in patients with CAVD compared to healthy volunteers ($p<0.01$; Figure 6C). These
414 patients had aortic valve sclerosis, which is an early stage of CAVD and characterized by
415 thickening and calcification of the aortic valve without obstruction of ventricular outflow
416 (Supplementary Figure I and Supplementary material Table III). There was no significant
417 difference in age and sex between healthy volunteers and CAVD patients. Body Mass Index
418 (BMI) was significantly decreased in CAVD patients compared to healthy volunteers ($p<0.05$,
419 Supplementary material Table III). A forward stepwise multivariate logistic analysis
420 (likelihood ratio) including zinc and BMI was performed. Increasing zinc serum levels was
421 shown to be a significant protective factor of CAVD after adjusted the BMI (OR=0.135; C.I.:
422 0.022~0.815; P=0.029). The statistical analysis are provided as Supplementary Methods.
423
424 **3.7 Reduction of GPR39 in calcified hVICs is blunted by zinc supplementation**
425 In agreement with our previous observations (Figure 6A and B), our *in vitro* studies
426 showed that GPR39 expression was also decreased at day 7 in calcified hVICs compared to
427 non-calcified hVICs, as demonstrated by immunofluorescence staining ($p<0.001$; Figure 7A)
428 and western blotting ($p<0.01$; Figure 7B). Interestingly, zinc supplementation significantly
429 attenuated the reduction of GPR39 in calcified hVICs (Figure 7A and 7B).
430
431 **4. Discussion**
432
433 The current study identifies that zinc as a novel inhibitor of CAVD. Zinc
434 supplementation significantly inhibits hVIC *in vitro* calcification, and this inhibitory effect is
435 abolished by the zinc chelator TPEN. Mechanistically, zinc supplementation inhibits
436 osteogenic differentiation and prevents apoptosis of hVICs, which is at least in part mediated
437 by GPR39-dependent ERK1/2 signaling pathway. Also, a significant reduction in the zinc
438 sensing receptor GPR39 expression in human calcified aortic valves is observed, and zinc
439 serum levels are decreased in patients with CAVD compared to healthy volunteers.
440 Furthermore, either knockdown of zinc transporter ZIP13 or ZIP14 reduced hVIC *in vitro*

441 calcification and osteogenic differentiation. This study provides direct evidence to show that
442 zinc supplementation inhibits the pathological process of CAVD, and highlights an important
443 role of ZIP13 and ZIP14 in the progression of CAVD.
444
445 Zinc, a vital trace element for normal health, is associated with a number of human
446 diseases, including cardiovascular disease, and diabetes. To our knowledge, the current study
447 is the first report indicating that zinc supplementation effectively inhibits hVIC *in vitro*
448 calcification. Zinc bioavailability is influenced by many factors in healthy individuals,
449 including zinc status of individuals, total zinc concentration and availability of soluble zinc in
450 the diet. The optimal serum zinc concentrations in adults are maintained between 13.8–22.9
451 μM[23]. We showed that 20 μM $ZnSO_4$ within this normal range was sufficient to inhibit
452 calcium deposition in hVICs. In addition, zinc is predominantly carried by serum albumin in
453 the blood[18]. Addition of serum albumin did not alter the inhibitory effect of zinc on hVIC *in*
454 *vitro* calcification. Our further analysis using TPEN chelator and $ZnCl_2$ confirmed the specific
455 inhibitory effect of zinc on calcification. Taken together, these data suggest that zinc is a key
456 inhibitor of CAVD.
457
458 Previous studies have shown that osteogenic transition of hVICs plays a crucial role in
459 the pathogenesis of CAVD[4, 8]. In the present study, zinc treatment significantly inhibited the
460 osteogenic gene *MSX2* and *ALPL* mRNA expression after 7 days. These data are consistent
461 with a recent study showing that zinc inhibits high phosphate-induced osteogenic transition of
462 human VSMCs[15]. However, zinc has previously been reported to enhance osteogenic
463 differentiation of human mesenchymal stem cells via up-regulation of RUNX2[24]. The
464 existence of cell-mediated differences may account for the different osteogenic responses
465 among these cells following zinc treatment.
466
467 Apoptosis is a key regulator of initiation and progression of CAVD[9-11]. Apoptotic bodies
468 expose phosphatidylserine on the outer membranes and generate a potential calcium-binding
469 site suitable for hydroxyapatite deposition[25, 26]. We showed that zinc attenuated apoptosis
470 during hVIC *in vitro* calcification process, but did not affect calcium phosphate precipitation.
471 Therefore, zinc-mediated inhibitory effect on hVIC calcification may involve inhibition of
472 apoptosis. These results also support previous reports demonstrating that zinc
473 supplementation prevents apoptosis in a number cell types including cardiomyocytes[27],
474 VSMCs[28], and in cardiac allografts[29]. In the present study, we showed that zinc
475 supplementation significantly attenuated *TNFα* mRNA expression during hVIC *in vitro*
476 calcification. TNFα, a pleiotropic cytokine, regulates a range of cellular activities including
477 proliferation, differentiation and apoptosis. TNFα-mediated signaling pathways have been
478 shown to play an important role in cardiovascular calcification[30, 31]. Furthermore, previous
479 studies have reported TNFα accelerates the calcification of hVICs through the BMP2-Dlx5
480 pathway[32]. Future studies are required to address whether the inhibitory effect of zinc on
481 hVIC calcification is mediated through down-regulation of TNFα or the reduced expression of
482 TNFα is just a consequence of cellular remodeling in calcification.
483
484 The human ZIP family functions to increase cytoplasmic zinc concentrations[22]. We

485 revealed that ZIP13 and ZIP14 were the most up-regulated ZIP family members in hVICs
486 following zinc treatment. ZIP13 is localized in intracellular vesicles and releases zinc from
487 vesicular stores[33]. We showed that knockdown of ZIP13 attenuated hVIC *in vitro* calcification,
488 and this inhibitory effect was further increased in the presence of zinc treatment. These results
489 suggest a zinc storage in intracellular vesicles plays a key role in hVIC *in vitro* calcification.
490 Interestingly, it has been reported that *Zip13* knockout mice show reduced osteogenesis and
491 abnormal cartilage development, which is mediated at least in part through TGF-β/bone
492 morphogenetic protein (BMP) signaling pathways[33]. In addition, ZIP13 has been shown to
493 suppress beige adipocyte biogenesis and energy expenditure by regulating c/ebp-beta
494 expression[34]. Consistent with this, knockdown of ZIP13 reduced osteogenic gene *MSX2* and
495 *ALPL* mRNA expression in hVICs. ZIP14 is responsible for zinc uptake by cells[35], and has
496 been reported to be a critical regulator of glucose homeostasis and beta-cell function[35, 36]. We
497 found that knockdown of ZIP14 in hVICs attenuated calcium deposition. However, this
498 inhibitory effect was abolished by zinc supplementation. This is likely due to a compensatory
499 role of other zinc transporters in uptake of zinc into cytoplasm from extracellular space when
500 additional zinc supplementation exists. Additionally, knockdown of ZIP14 decreased
501 *MSX2* mRNA expression in hVICs, suggesting ZIP14-mediated zinc uptake may regulate
502 osteogenic differentiation of hVICs. Taken together, our data expand upon these findings and
503 highlight the important role of ZIP13 and ZIP14 in the maintenance of intracellular zinc
504 homeostasis in hVIC *in vitro* calcification and their potential roles in CAVD. The mechanisms
505 underlying the anti-calcific effects of ZIP13 or ZIP14 silencing are currently elusive and
506 require further study.
507
508 It should be noted that extracellular zinc and intracellular zinc have opposite role in the
509 regulation of hVIC calcification and osteogenic differentiation. Extracellular zinc may signal
510 through GPR39 to activate a number of intracellular signaling pathways[21], thereby regulating
511 hVIC calcification and osteogenic differentiation. However, intracellular zinc mediated by
512 zinc transporters may act as co-factors for a number of enzymes such as ALPL[37], which play
513 an important role in hVIC calcification and osteogenic differentiation.
514
515 In order to characterize the underlying mechanisms through which zinc exerts its
516 protective on hVICs, the PI3-kinase/AKT and MAPK/ERK1/2 signaling pathways were
517 investigated. These pathways play an important role in a wide range of cellular functions,
518 including cell proliferation, cell survival, and calcification[38, 39]. We showed that zinc treatment
519 only induced the phosphorylation of ERK1/2 in hVICs, which is consistent with previous
520 reports showing that activation of this pathway by zinc in skeletal muscle cells[40], myogenic
521 cells[41], and colonocytes[42]. In contrast to these studies, no induction of AKT phosphorylation
522 by zinc was observed in hVICs. We also demonstrated that either pharmacological or
523 siRNA-mediated inhibition of ERK1/2 signaling pathway significantly blunted the protective
524 effect of zinc on hVIC *in vitro* calcification and apoptosis. Indeed, the ERK1/2 signaling
525 pathway has been shown to regulate calcification in osteoblasts[43], VSMCs[44], and human
526 VICs[45]. However, some previous studies have reported that the activation of ERK1/2
527 signaling pathway exerts pro-calcific effects in valvular calcification. The disparate findings
528 between our studies and theirs may result from different pro-calcific environments (that is

529 high calcium and phosphate vs. fibrin and tissue culture polystyrene) and species (human vs.
530 porcine)[19]. In addition, inhibition of ERK1/2 signaling pathway has been shown to attenuate
531 aortic valve disease processes in an Emilin1-deficient mouse model[46]. The abnormalities of
532 aortic valves in these mice include early elastic fiber fragmentation and aberrant angiogenesis,
533 however no aortic valve calcification was detected at any stage[46, 47]. Further investigations are
534 required to examine the effects of zinc-mediated ERK1/2 signaling pathway on aortic valve
535 calcification using mouse models of CAVD. Taken together, our data confirms and extends
536 these previous reports indicating the importance of the ERK1/2 signaling pathway in the
537 regulation of CAVD.
538
539 GPR39 has been functionally characterized as a zinc-dependent, G-protein coupled
540 receptor that senses changes in extracellular zinc and mediates zinc dependent cellular
541 signaling pathways[48]. It is widely expressed by a number of cell types including vascular
542 endothelial cells and VSMCs[15, 21]. We extended on these previous studies showing that
543 GPR39 is expressed by hVICs, and silencing of GPR39 abrogated zinc activation of ERK1/2
544 signaling pathway. We also showed that inhibition of ERK signaling pathway attenuated
545 zinc-mediated inhibitory effect on hVIC apoptosis and calcification. In addition, knockdown
546 of GPR39 blunted the inhibitory effect of zinc supplementation on hVIC *in vitro* calcification,
547 osteogenic differentiation and apoptosis. Taken together, these data support that zinc signals
548 through GPR39 to activate ERK1/2 signaling pathway, thereby suppressing osteogenic
549 differentiation and apoptosis, which could inhibit hVIC calcification.
550
551 The most important observation in this study was that the zinc sensing receptor GPR39
552 expression was decreased in calcified hVICs and human aortic valves from patients with
553 CAVD. The pathological role of GPR39 deficiency has been previously described. Deletion of
554 GPR39 in mice results in zinc deficiency symptoms including depression, accelerated gastric
555 emptying, and increased fecal excretion[49]. Furthermore, GPR39 knockout mice display
556 enhanced high fat-induced obesity due to altered adipocyte metabolism[50]. Interestingly, we
557 observed that zinc treatment prevented the reduction of GPR39 in calcified hVICs. This is in
558 consistent with a previous report showing that zinc deficiency reduces expression of the
559 GPR39 receptor in the mouse frontal cortex[51]. These data raise the possibility that zinc
560 supplementation may reverse aortic valve calcification. It would be interesting to investigate
561 whether zinc supplementation could reverse the established aortic valve calcification in mouse
562 models of CAVD. Nonetheless, our data provide novel evidence that support a key role of
563 GPR39 deficiency in the pathogenesis of CAVD.
564
565 Reduced zinc levels are commonly seen in patients with chronic kidney disease (CKD)[52].
566 In addition, reduced zinc serum levels are also associated with carotid artery atherosclerosis in
567 hemodialysis patients[53]. Interestingly, a recent study has shown that zinc serum concentrations
568 inversely correlated with serum calcification propensity in CKD patients[15]. In accordance
569 with these studies, we observed a significant reduction in zinc serum levels in a cohort of
570 Chinese CAVD patients compared to healthy volunteers. These data together with our hVIC *in*
571 *vitro* calcification studies highlight the important inhibitory role of zinc in the development of
572 CAVD.

It should be noted that this study may contain some limitations. The hVICs used in the present study were isolated from diseased aortic valve tissues, which may be more sensitive to apoptosis and cell death. In addition, the inhibitory or reversal effect of zinc on CAVD was not tested *in vivo*. Future studies are required to investigate whether zinc supplementation can inhibit or reverse aortic valve calcification using mouse models of CAVD.

In conclusion, we report that zinc as a novel inhibitor of CAVD. The zinc sensing receptor GPR39 is reduced in calcified aortic valves from patients with CAVD. The anti-calcific effect of zinc on hVIC calcification is at least in part mediated through inhibition of apoptosis and osteogenic differentiation via GPR39 dependent EKR1/2 signaling pathway. Our study also highlights an important role of zinc transporter ZIP13 and ZIP14 in CAVD. This work warrants further investigations of zinc supplementation or zinc transporter ZIP13 and ZIP14 as a potential novel therapeutic strategy for treatment of CAVD.

Supplementary material

Supplementary material is available at Cardiovascular Research online.

Funding

This work was supported by funding from the National Natural Science Foundation for Young Scientists of China (No. 81800428 to D. Zhu), The Innovation Project of Department of Education of Guangdong Province (No. 2017KTSCX158 to D. Zhu), Guangdong Natural Science Foundation (No. 2018A030310178 to D. Zhu), Science and Technology Projects of Guangzhou (No. 201904010289 to D. Zhu), Science and Technology Projects of Guangzhou (No.201903010005 to L. Jiang). We are also grateful to the Dr Lawrence Ho Research and Development Fund to K. Staines and D. Zhu.

Author contributions: ZC, FG-M, and LJ performed the majority of experiments. PH, WH, and XW performed some of the experiments. KAS, VEM, CZ, DY and XF revised the manuscript. ZC, FG-M, and DZ designed the experiments. DZ supervised the whole work and wrote the manuscript. All authors read and accepted the manuscript.

Acknowledgments

None.

Conflict of interest

None.

References

1. Rajamannan NM, Evans FJ, Aikawa E, Grande-Allen KJ, Demer LL, Heistad DD, Simmons CA, Masters KS, Mathieu P, O'Brien KD, Schoen FJ, Towler DA, Yoganathan AP, Otto CM. Calcific aortic valve disease: Not simply a degenerative process: A review and agenda for research from the national heart and lung and blood institute aortic stenosis working group. Executive summary: Calcific aortic valve disease-2011 update. *Circulation* 2011;**124**:1783-1791.

2. Sehatzadeh S, Doble B, Xie F, Blackhouse G, Campbell K, Kaulback K, Chandra K, Goeree R. Transcatheter aortic valve implantation (tavi) for treatment of aortic valve stenosis: An evidence update. *Ont Health Technol Assess Ser* 2013;**13**:1-40.
3. Rodriguez-Gabella T, Voisine P, Puri R, Pibarot P, Rodes-Cabau J. Aortic Bioprosthetic Valve Durability: Incidence, Mechanisms, Predictors, and Management of Surgical and Transcatheter Valve Degeneration. *J Am Coll Cardiol* 2017;**70**:1013-1028.
4. Guauque-Olarte S, Messika-Zeitoun D, Droit A, Lamontagne M, Tremblay-Marchand J, Lavoie-Charland E, Gaudreault N, Arsenault BJ, Dube MP, Tardif JC, Body SC, Seidman JG, Boileau C, Mathieu P, Pibarot P, Bosse Y. Calcium signaling pathway genes runx2 and cacna1c are associated with calcific aortic valve disease. *Circ Cardiovasc Genet* 2015;**8**:812-822.
5. Rattazzi M, Bertacco E, Del Vecchio A, Puato M, Faggin E, Pauletto P. Aortic valve calcification in chronic kidney disease. *Nephrol Dial Transplant* 2013;**28**:2968-2976.
6. Umana E, Ahmed W, Alpert MA. Valvular and perivalvular abnormalities in end-stage renal disease. *Am J Med Sci* 2003;**325**:237-242.
7. Hadji F, Boulanger M. C, Guay S. P, Gaudreault N, Amellah S, Mkannez G, Bouchareb R, Marchand J. T, Nsaibia M. J, Guauque-Olarte S, Pibarot P, Bouchard L, Bossé Y, Mathieu P. Altered DNA Methylation of Long Noncoding RNA H19 in Calcific Aortic Valve Disease Promotes Mineralization by Silencing NOTCH1. *Circulation* 2016;**134**: 1848-1862.
8. Cui L, Rashdan NA, Zhu D, Milne EM, Ajuh P, Milne G, Helfrich MH, Lim K, Prasad S, Lerman DA, Vesey AT, Dweck MR, Jenkins WS, Newby DE, Farquharson C, Macrae VE. End stage renal disease-induced hypercalcemia may promote aortic valve calcification via annexin vi enrichment of valve interstitial cell derived-matrix vesicles. *J Cell Physiol* 2017;**232**:2985-2995.
9. Galeone A, Brunetti G, Oranger A, Greco G, Di Benedetto A, Mori G, Colucci S, Zallone A, Paparella D, Grano M. Aortic valvular interstitial cells apoptosis and calcification are mediated by tnf-related apoptosis-inducing ligand. *Int J Cardiol* 2013;**169**:296-304.
10. Jian B, Narula N, Li QY, Mohler ER, 3rd, Levy RJ. Progression of aortic valve stenosis: Tgf-beta1 is present in calcified aortic valve cusps and promotes aortic valve interstitial cell calcification via apoptosis. *Ann Thorac Surg* 2003;**75**:457-465.
11. Cote N, El Husseini D, Pepin A, Guauque-Olarte S, Ducharme V, Bouchard-Cannon P, Audet A, Fournier D, Gaudreault N, Derbali H, McKee MD, Simard C, Despres JP, Pibarot P, Bosse Y, Mathieu P. Atp acts as a survival signal and prevents the mineralization of aortic valve. *J Mol Cell Cardiol* 2012;**52**:1191-1202.
12. Beattie JH, Gordon MJ, Duthie SJ, McNeil CJ, Horgan GW, Nixon GF, Feldmann J, Kwun IS. Suboptimal dietary zinc intake promotes vascular inflammation and atherogenesis in a mouse model of atherosclerosis. *Mol Nutr Food Res* 2012;**56**:1097-1105.
13. Jenner A, Ren M, Rajendran R, Ning P, Huat BT, Watt F, Halliwell B. Zinc supplementation inhibits lipid peroxidation and the development of atherosclerosis in rabbits fed a high cholesterol diet. *Free Radic Biol Med* 2007;**42**:559-566.
14. Yan YW, Fan J, Bai SL, Hou WJ, Li X, Tong H. Zinc prevents abdominal aortic aneurysm formation by induction of a20-mediated suppression of nf-kappab pathway.

PloS One 2016;**11**:e0148536.

15. Voelkl J, Tuffaha R, Luong TTD, Zickler D, Masyout J, Feger M, Verheyen N, Blaschke F, Kuro OM, Tomaschitz A, Pilz S, Pasch A, Eckardt KU, Scherberich JE, Lang F, Pieske B, Alesutan I. Zinc inhibits phosphate-induced vascular calcification through tnfaip3-mediated suppression of nf-kappab. *J Am Soc Nephrol* 2018;**29**:1636-1648.
16. Lis GJ, Czapla-Masztafiak J, Kwiatek WM, Gajda M, Jasek E, Jasinska M, Czubek U, Borchert M, Appel K, Nessler J, Sadowski J, Litwin JA. Distribution of selected elements in calcific human aortic valves studied by microscopy combined with sr-muxrf: Influence of lipids on progression of calcification. *Micron* 2014;**67**:141-148.
17. von Elm E, Altman DG, Egger M, Pocock JS, Gøtzsche PC, Vandenbroucke JP, STROBE Initiative. The Strengthening theReporting of Observational Studies in Epidemiology (STROBE) statement: guidelines for reporting observational studies. *PLoS Med* 2007; **4**:e296.
18. Handing KB, Shabalin IG, Kassaar O, Khazaipoul S, Blindauer CA, Stewart AJ, Chruszcz M, Minor W. Circulatory zinc transport is controlled by distinct interdomain sites on mammalian albumins. *Chem Sci* 2016;**7**:6635-6648.
19. Gu X, Masters KS. Role of the mapk/erk pathway in valvular interstitial cell calcification. *Am J Physiol Heart Circ Physiol* 2009;**296**:H1748-1757.
20. Yuan ZS, Zhou YZ, Liao XB, Luo JW, Shen KJ, Hu YR, Gu L, Li JM, Tan CM, Chen HM, Zhou XM. Apelin attenuates the osteoblastic differentiation of aortic valve interstitial cells via the erk and pi3-k/akt pathways. *Amino Acids* 2015;**47**:2475-2482.
21. Zhu D, Su Y, Zheng Y, Fu B, Tang L, Qin YX. Zinc regulates vascular endothelial cell activity through zinc-sensing receptor znr/gpr39. *Am J Physiol Cell Physiol* 2018;**314**:C404-C414.
22. Bafaro E, Liu Y, Xu Y, Dempski RE. The emerging role of zinc transporters in cellular homeostasis and cancer. *Signal Transduct Target Ther* 2017;**2**:17029.
23. Paul S, Prashant A, T RC, Suma MN, Vishwanath P, R ND. The micronutrient levels in the third trimester of pregnancy and assessment of the neonatal outcome: a pilot study. *J Clin Diagn Res* 2013;**7**:1572-1575.
24. Park KH, Choi Y, Yoon DS, Lee KM, Kim D, Lee JW. Zinc promotes osteoblast differentiation in human mesenchymal stem cells via activation of the camp-pka-creb signaling pathway. *Stem Cells Dev* 2018;**27**:1125-1135.
25. Proudfoot D, Skepper JN, Hegyi L, Bennett MR, Shanahan CM, Weissberg PL. Apoptosis regulates human vascular calcification in vitro: Evidence for initiation of vascular calcification by apoptotic bodies. *Circ Res* 2000;**87**:1055-1062.
26. Skrtic D, Eanes ED. Membrane-mediated precipitation of calcium phosphate in model liposomes with matrix vesicle-like lipid composition. *Bone Miner* 1992;**16**:109-119.
27. Kumar SD, Vijaya M, Samy RP, Dheen ST, Ren M, Watt F, Kang YJ, Bay BH, Tay SS. Zinc supplementation prevents cardiomyocyte apoptosis and congenital heart defects in embryos of diabetic mice. *Free Radic Biol Med* 2012;**53**:1595-1606.
28. Allen-Redpath K, Ou O, Beattie JH, Kwun IS, Feldmann J, Nixon GF. Marginal dietary zinc deficiency in vivo induces vascular smooth muscle cell apoptosis in large arteries. *Cardiovasc Res* 2013;**99**:525-534.
29. Kown MH, Van der Steenhoven T, Blankenberg FG, Hoyt G, Berry GJ, Tait JF, Strauss

705 HW, Robbins RC. Zinc-mediated reduction of apoptosis in cardiac allografts. *Circulation*
706 2000;**102**:III228-232.
707 30. Tintut Y, Patel J, Parhami F, Demer LL. Tumor necrosis factor-alpha promotes in vitro
708 calcification of vascular cells via the cAMP pathway. *Circulation* 2000;**102**:2636-2642.
709 31. Zickler D, Luecht C, Willy K, Chen L, Witowski J, Girndt M, Fiedler R, Storr M,
710 Kamhieh-Milz J, Schoon J, Geissler S, Ringdén O, Schindler R, Moll G, Dragun D, Catar
711 R**.** Tumour necrosis factor-alpha in uraemic serum promotes osteoblastic transition and
712 calcification of vascular smooth muscle cells via extracellular signal-regulated kinases
713 and activator protein 1/c-FOS-mediated induction of interleukin 6 expression. *Nephrol*
714 *Dial Transplant* **2018**;33:574-585.
715 32. Yu Z, Seya K, Daitoku K, Motomura S, Fukuda I, Furukawa K. Tumor necrosis
716 factor-alpha accelerates the calcification of human aortic valve interstitial cells obtained
717 from patients with calcific aortic valve stenosis via the BMP2-Dlx5 pathway. *J*
718 *Pharmacol Exp Ther* **2011**;337:16-23.
719 33. Fukada T, Civic N, Furuichi T, Shimoda S, Mishima K, Higashiyama H, Idaira Y, Asada Y,
720 Kitamura H, Yamasaki S, Hojyo S, Nakayama M, Ohara O, Koseki H, Dos Santos HG,
721 Bonafe L, Ha-Vinh R, Zankl A, Unger S, Kraenzlin ME, Beckmann JS, Saito I, Rivolta C,
722 Ikegawa S, Superti-Furga A, Hirano T. The zinc transporter slc39a13/zip13 is required for
723 connective tissue development; its involvement in bmp/tgf-beta signaling pathways. *PloS*
724 *One* 2008;**3**:e3642.
725 34. Fukunaka A, Fukada T, Bhin J, Suzuki L, Tsuzuki T, Takamine Y, Bin BH, Yoshihara T,
726 Ichinoseki-Sekine N, Naito H, Miyatsuka T, Takamiya S, Sasaki T, Inagaki T, Kitamura T,
727 Kajimura S, Watada H, Fujitani Y. Zinc transporter zip13 suppresses beige adipocyte
728 biogenesis and energy expenditure by regulating c/ebp-beta expression. *PLoS Genet*
729 2017;**13**:e1006950.
730 35. Maxel T, Smidt K, Petersen CC, Honore B, Christensen AK, Jeppesen PB, Brock B,
731 Rungby J, Palmfeldt J, Larsen A. The zinc transporter zip14 (slc39a14) affects beta-cell
732 function: Proteomics, gene expression, and insulin secretion studies in ins-1e cells. *Sci*
733 *Rep* 2019;**9**:8589.
734 36. Aydemir TB, Troche C, Kim MH, Cousins RJ. Hepatic zip14-mediated zinc transport
735 contributes to endosomal insulin receptor trafficking and glucose metabolism. *J Biol*
736 *Chem* 2016;**291**:23939-23951.
737 37. Mornet E, Stura E, Lia-Baldini AS, Stigbrand T, Menez A, Le Du MH. Structural
738 evidence for a functional role of human tissue nonspecific alkaline phosphatase in bone
739 mineralization. *J Biol Chem* 2001;**276**:31171-31178.
740 38. Gharibi B, Ghuman MS, Hughes FJ. Akt- and erk-mediated regulation of proliferation
741 and differentiation during pdgfrbeta-induced msc self-renewal. *J Cell Mol Med*
742 2012;**16**:2789-2801.
743 39. Byon CH, Javed A, Dai Q, Kappes JC, Clemens TL, Darley-Usmar VM, McDonald JM,
744 Chen Y. Oxidative stress induces vascular calcification through modulation of the
745 osteogenic transcription factor runx2 by akt signaling. *J Biol Chem*
746 2008;**283**:15319-15327.
747 40. Norouzi S, Adulcikas J, Sohal SS, Myers S. Zinc stimulates glucose oxidation and
748 glycemic control by modulating the insulin signaling pathway in human and mouse

749 skeletal muscle cell lines. *PloS One* 2018;**13**:e0191727.
750 41. Ohashi K, Nagata Y, Wada E, Zammit PS, Shiozuka M, Matsuda R. Zinc promotes
751 proliferation and activation of myogenic cells via the pi3k/akt and erk signaling cascade.
752 *Exp Cell Res* 2015;**333**:228-237.
753 42. Cohen L, Sekler I, Hershfinkel M. The zinc sensing receptor, znr/gpr39, controls
754 proliferation and differentiation of colonocytes and thereby tight junction formation in the
755 colon. *Cell Death Dis* 2014;**5**:e1307.
756 43. Ge C, Xiao G, Jiang D, Franceschi RT. Critical role of the extracellular signal-regulated
757 kinase-mapk pathway in osteoblast differentiation and skeletal development. *J Cell Biol*
758 2007;**176**:709-718.
759 44. Zhu D, Mackenzie NC, Millan JL, Farquharson C, MacRae VE. A protective role for
760 fgf-23 in local defence against disrupted arterial wall integrity? *Mol Cell Endocrinol*
761 2013;**372**:1-11.
762 45. Rosa M, Paris C, Sottejeau Y, Corseaux D, Robin E, Tagzirt M, Juthier F, Jashari R,
763 Rauch A, Vincentelli A, Staels B, Van Belle E, Susen S, Dupont A. Leptin induces
764 osteoblast differentiation of human valvular interstitial cells via the akt and erk pathways.
765 *Acta Diabetol* 2017;**54**:551-560.
766 46. Munjal C, Jegga AG, Opoka AM, Stoilov I, Norris RA, Thomas CJ, Smith JM, Mecham
767 RP, Bressan GM, Hinton RB, . Inhibition of MAPK-Erk pathway in vivo attenuates aortic
768 valve disease processes in Emilin1-deficient mouse model. *Physiol Rep* 2017;**5**:pii:
769 e13152.
770 47. Munjal C, Opoka AM, Osinska H, James JF, Bressan GM, Hinton RB. TGF-beta
771 mediates early angiogenesis and latent fibrosis in an Emilin1-deficient mouse model of
772 aortic valve disease. *Dis Model Mech* 2014;7:987-996.
773 48. Hershfinkel M, Moran A, Grossman N, Sekler I. A zinc-sensing receptor triggers the
774 release of intracellular ca2+ and regulates ion transport. *Proc Natl Acad Sci U S A*
775 2001;**98**:11749-11754.
776 49. Mlyniec K, Budziszewska B, Holst B, Ostachowicz B, Nowak G. Gpr39 (zinc receptor)
777 knockout mice exhibit depression-like behavior and creb/bdnf down-regulation in the
778 hippocampus. *Int J Neuropsycho pharmacol* 2014;**18**:pyu002.
779 50. Petersen PS, Jin C, Madsen AN, Rasmussen M, Kuhre R, Egerod KL, Nielsen LB,
780 Schwartz TW, Holst B. Deficiency of the gpr39 receptor is associated with obesity and
781 altered adipocyte metabolism. *FASEB J* 2011;**25**:3803-3814.
782 51. Mlyniec K, Budziszewska B, Reczynski W, Sowa-Kucma M, Nowak G. The role of the
783 gpr39 receptor in zinc deficient-animal model of depression. *Behav Brain Res*
784 2013;**238**:30-35.
785 52. Damianaki K, Lourenco JM, Braconnier P, Ghobril JP, Devuyst O, Burnier M, Lenglet S,
786 Augsburger M, Thomas A, Pruijm M. Renal handling of zinc in chronic kidney disease
787 patients and the role of circulating zinc levels in renal function decline. *Nephrol Dial*
788 *Transplant* 2019.
789 53. Ari E, Kaya Y, Demir H, Asicioglu E, Keskin S. The correlation of serum trace elements
790 and heavy metals with carotid artery atherosclerosis in maintenance hemodialysis patients.
791 *Biol Trace Elem Res* 2011;**144**:351-359.
792

Figure legends

Figure 1. Zinc inhibits hVICs *in vitro* calcification and osteogenic differentiation. hVICs were exposed to control (Ctr), calcification media (Cal), $ZnSO_4$ with or without TPEN, $ZnCl_2$, and $ZnSO_4$ with or without albumin for up to 7 days as indicated. A. Representative alizarin red S staining images at day 7 (n=3). Plate view (upper) and microscopic view (lower), scale bar 100 μm. B. Quantitative calcium assay showed that $ZnSO_4$ inhibited hVIC *in vitro* calcification at day 7 (n=4). C. Representative confocal images of FluoZin-3 staining at day 3 and day 7 (n=3). Scale bar 50 μm. D. Quantitative calcium assay showed that 10 μM TPEN blunted the inhibitory effect of $ZnSO_4$ on hVIC *in vitro* calcification at day 7 (n=4). E. Quantitative calcium assay at day 7 (n=4). F and G. Quantitative RT-PCR for *MSX2* and *ALPL* mRNA expression in hVICs cultured with calcifying media after 7 days (n=6). H. Quantitative calcium assay showed that albumin did not affect the inhibitory effect of $ZnSO_4$ on hVIC *in vitro* calcification (n=4). Results are presented as mean ± SEM. ANOVA by Bonferroni post-test, $^{*}p < 0.05$, $^{***}p < 0.001$ compared to control, $^{\#}p<0.05$, $^{\#\#}p<0.01$, $^{\#\#\#}p < 0.001$ compared to calcification. $^{+++}p < 0.001$ compared to calcification with zinc treatment.

Figure 2. Zinc prevents apoptosis of hVICs under calcifying conditions. hVICs were exposed to control (Ctr) or calcification media (Cal) with or without 20 μM of $ZnSO_4$ treatment. A. Cell death at day 3 and day 7 (n=6). B. Representative apoptotic nuclei images of DAPI staining (left panel) and quantitative analysis of the percentage of apoptotic cells (right panel). White arrows indicate apoptotic cells, scale bar 10 μm (n=11). C. Flow cytometry analysis of Annexin V and Propidium Iodide (PI) staining (upper panels) and quantification of the percentage of early apoptotic cells (Q3, lower panel) at day 3 (n=3). D. Representative western blot of Caspase 3, cleaved Caspase 3, and β-actin (n=4). E. Calcium phosphate precipitation analysis showed that $ZnSO_4$ did not affect calcium/phosphate deposition (n=4). F. Quantitative RT-PCR for *TNFα* mRNA expression in hVICs cultured with calcifying media after 7 days (n=6). G. Quantitative RT-PCR for *TGFβ* mRNA expression (n=5 or 6). Results are presented as mean ± SEM. ANOVA by Bonferroni post-test. $^{*}p < 0.05$, $^{**}p < 0.01$, $^{***}p < 0.001$ compared to control. $^{\#}p < 0.05$, $^{\#\#}p < 0.01$, $^{\#\#\#}p < 0.001$ compared to calcification.

Figure 3. Zinc inhibits hVICs calcification and apoptosis through activation of the ERK1/2 signaling pathway. hVICs were exposed to control (Ctr), calcification media (Cal), 20 μM $ZnSO_4$ treatment with or without 10 μM ERK inhibitor (PD98059) or siERK1/2 as indicated. A. hVICs were exposed to $ZnSO_4$ for 10, 30, and 60 minutes. Representative western blot of phospho-AKT (p-AKT), total AKT, phospho-ERK (p-ERK), total ERK, and β-actin (left panel) and quantification of the relative protein expression (right panel) (n=4). B. Representative alizarin red S staining images at day 7 (n=3). Plate view (upper) and microscopic view (lower), scale bar 100 μm. C. Quantitative calcium assay at day 7 (n=4). D. Representative Western blot of Caspase 3, cleaved Caspase 3, and β-actin (n=4). E. Cell death at day 7 (n=6). F. Quantitative calcium assay at Day7 (n=4). Results are presented as mean ± SEM. ANOVA by Bonferroni post-test. $^{*}p < 0.05$, $^{**}p < 0.01$, $^{***}p < 0.001$ compared to control. $^{\#}p < 0.05$, $^{\#\#\#}p < 0.001$ compared to calcification, $^{+}p < 0.05$, $^{++}p < 0.01$ compared to

837 calcification with zinc treatment.
838
839 **Figure 4. Zinc signals through the zinc-sensing receptor GRR39 to inhibit hVICs**
840 **calcification.** hVICs were transfected with GPR39 siRNA (siGPR39) or negative control
841 siRNA (siNC) and exposed to control (Ctr), calcification media (Cal) with or without 20 μM
842 of $ZnSO_4$ treatment. A. Representative western blot of GPR39 from 5 independent hVICs
843 isolation. B. GPR39 silencing efficiency using three different siRNA (n=3). GPR39 siRNA 2
844 was selected for subsequent experiments. C. Representative western blot of phospho-AKT
845 (p-AKT), total AKT, phospho-ERK (p-ERK), total ERK, and β-actin after 30 minutes with
846 $ZnSO_4$ (n=4). D. Representative alizarin red S staining images at day 7 (n=3). Plate view
847 (upper) and microscopic view (lower), scale bar 100 μm. E. Quantitative analysis of calcium
848 content at day 7 (n=5). F. Representative western blot of Caspase 3, cleaved Caspase 3, and
849 β-actin (n=4). G-I. Relative mRNA expression of *MSX2*, *BMP2* and *RUNX2* (n=6). Results
850 are presented as mean ± SEM. ANOVA by Bonferroni post-test. *$p < 0.05$, **$p < 0.01$, ***$p <$
851 0.001 compared to control plus siNC. $^{\#}p < 0.05$, $^{\#\#}p < 0.01$, $^{\#\#\#}p < 0.001$ compared to
852 calcification plus siNC. $^{+}p < 0.05$, $^{+++}p < 0.001$ compared to calcification with zinc treatment
853 plus siNC.
854
855 **Figure 5. Knockdown of ZIP13 or ZIP14 inhibits hVIC *in vitro* calcification and**
856 **osteogenic differentiation.** hVICs were exposed to control (Ctr), or 20 μM $ZnSO_4$ treatment
857 for 2 days, or transfected with siZIP13 or siZIP14, and exposed to calcification media (Cal) or
858 20 μM ZnSO4 treatment for up to 7 days as indicated. A. Relative mRNA expression of zinc
859 transporter ZIP1-14 was examined by quantitative RT-PCR (n=6 or 8), unpaired Student's
860 t-test. B. Representative alizarin red S staining images for hVICs transfected with siZIP13 at
861 day 7 (n=3). C. Quantitative analysis of calcium content for hVICs transfected with siZIP13 at
862 day 7 (n=5), ANOVA by Bonferroni post-test. D. Representative alizarin red S staining
863 images for hVICs transfected with siZIP14 at day 7 (n=3). E. Quantitative analysis of calcium
864 content for hVICs transfected with siZIP14 at day 7 (n=5), ANOVA by Bonferroni post-test.
865 F-G. Relative mRNA expression of *MSX2* and *BMP2* at Day 7 (n=8). ANOVA by Bonferroni
866 post-test. H-I. Representative confocal images of FluoZin-3 staining at day 7 and quantitative
867 analysis of zinc fluorescence intensity (n=6), ANOVA by Bonferroni post-test. Scale bar 50
868 μm. Results are presented as mean ± SEM. *$p<0.05$, **<0.01, ***$p < 0.001$ compared to
869 control. $^{\#}p < 0.05$, $^{\#\#\#}p< 0.001$ compared to calcification plus siNC. $^{+}p<0.05$, $^{++}p < 0.01$, ^{+++}p
870 < 0.001 compared to calcification with zinc treatment plus siNC.
871
872 **Figure 6. GPR39 expression is down-regulated in calcified human aortic valves.** A.
873 Immunohistologic evaluation of GPR39 expression in non-calcified and calcified human
874 aortic valves (n=3). B. Representative western blot of GPR39 expression from 4 non-calcified
875 or calcified human aortic valves (upper panels) and relative GPR39 expression (lower panel)
876 (n=4), unpaired Student's t-test. C. Serum zinc concentrations in healthy and CAVD patients
877 (n=15), Mann-Whitney test. Results are presented as mean ± SEM. *$p < 0.05$, **$p < 0.01$
878 compared to control.
879
880 **Figure 7. Zinc treatment prevents the down-regulation of GPR39 induced by**

881 **calcification *in vitro*.** hVICs were exposed to control (Ctr) or calcification media (Cal) with
882 or without additional 20 μM of $ZnSO_4$ at day 3 and day 7. A. Representative confocal images
883 of GPR39 immunostaining and relative GPR39 fluorescence intensity (lower panel) (n=8),
884 ANOVA by Bonferroni post-test. B. Western blot of GPR39 expression (upper panel) and
885 relative GPR39 expression (lower panel) (n=4), ANOVA by Bonferroni post-test. Results are
886 presented as mean ± SEM. *$p < 0.05$, **$p < 0.01$, **$p < 0.001$ compared to control. $^{\#}p < 0.05$,
887 $^{\#\#}p < 0.01$ compared to calcification.

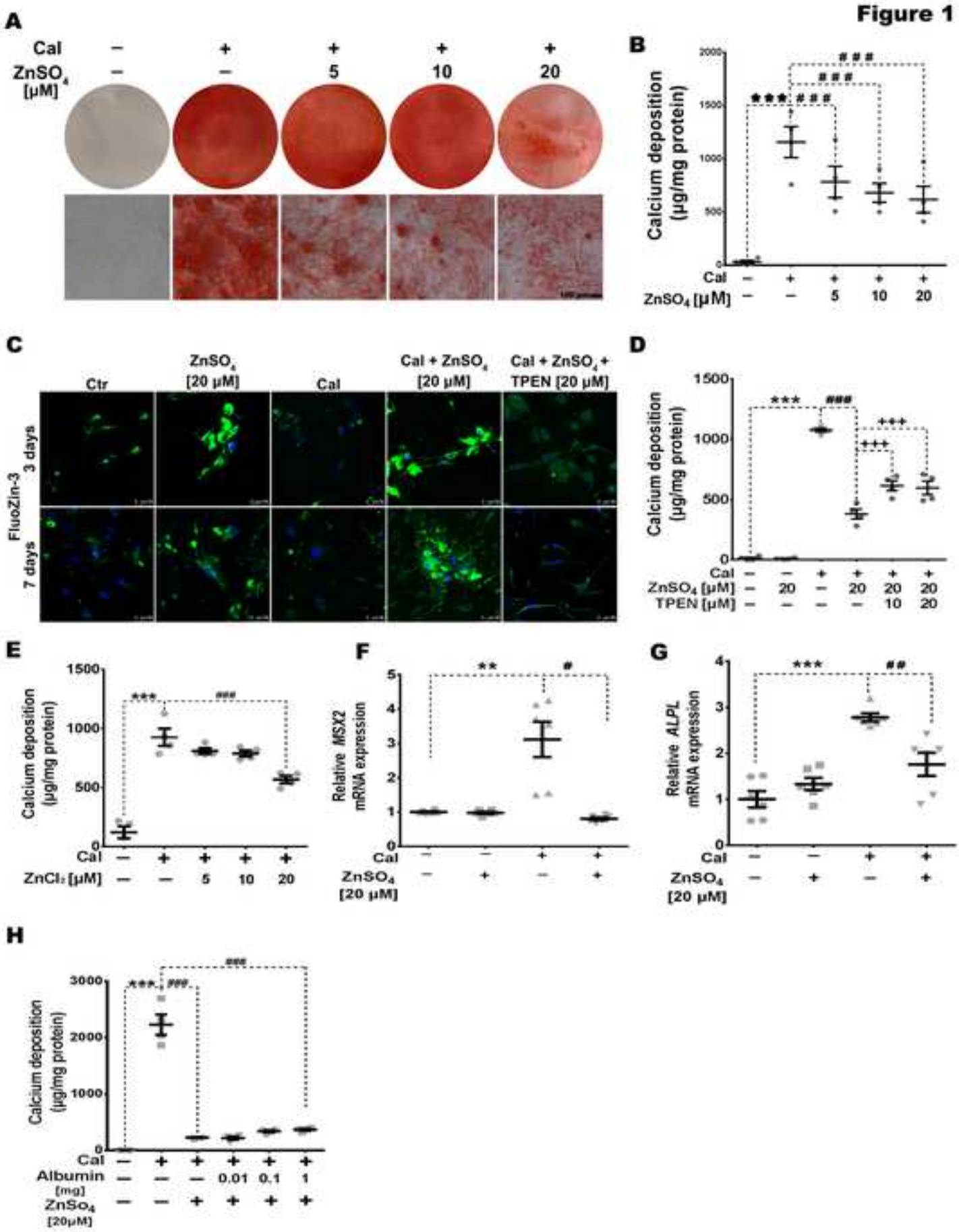
Figure 1
A
Cal
ZnSO4 [μM]
B
Calcium deposition (μg/mg protein)
Cal
ZnSO4 [μM]
C
Ctr
ZnSO4 [20 μM]
Cal
Cal + ZnSO4 [20 μM]
Cal + ZnSO4 + TPEN [20 μM]
FluoZin-3
3 days
7 days
D
Calcium deposition (μg/mg protein)
Cal
ZnSO4 [μM]
TPEN [μM]
E
Calcium deposition (μg/mg protein)
Cal
ZnCl2 [μM]
F
Relative MSX2 mRNA expression
Cal
ZnSO4 [20 μM]
G
Relative ALPL mRNA expression
Cal
ZnSO4 [20 μM]
H
Calcium deposition (μg/mg protein)
Cal
Albumin [mg]
ZnSo4 [20μM]

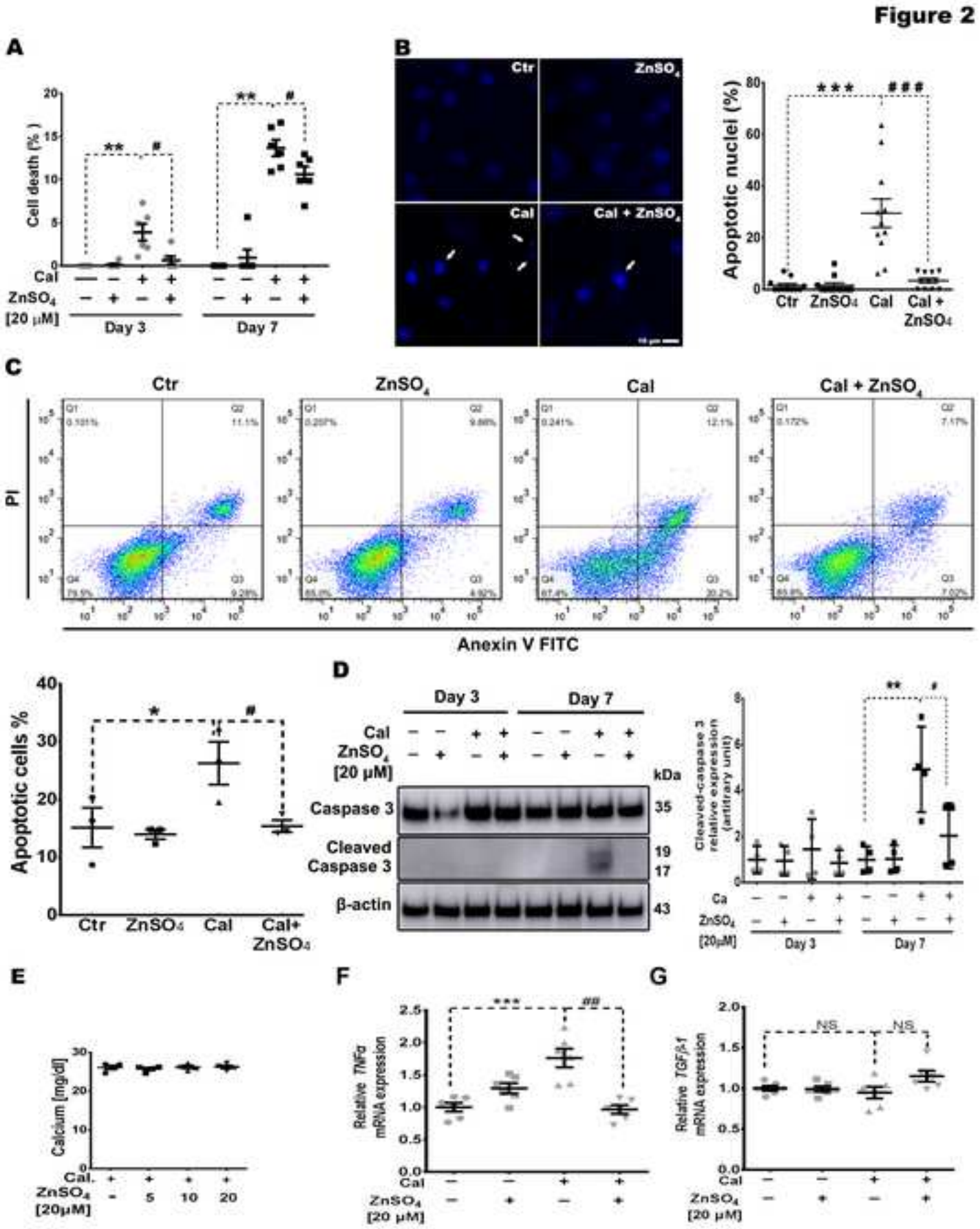
Figure 2
A
Cell death (%)
Cal
ZnSO4
[20 μM]
Day 3
Day 7
B
Ctr
ZnSO4
Cal
Cal + ZnSO4
Apoptotic nuclei (%)
Ctr
ZnSO4
Cal
Cal + ZnSO4
C
Ctr
ZnSO4
Cal
Cal + ZnSO4
PI
Anexin V FITC
Apoptotic cells %
Ctr
ZnSO4
Cal
Cal+ ZnSO4
D
Day 3
Day 7
Cal
ZnSO4
[20 μM]
kDa
Caspase 3
Cleaved Caspase 3
β-actin
35
19
17
43
Cleaved-caspase 3 relative expression (arbitrary unit)
Ca
ZnSO4
[20μM]
Day 3
Day 7
E
Calcium [mg/dl]
Cal.
ZnSO4
[20μM]
5
10
20
F
Relative TNFα mRNA expression
Cal
ZnSO4
[20 μM]
G
Relative TGFβ1 mRNA expression
NS
NS
Cal
ZnSO4
[20 μM]

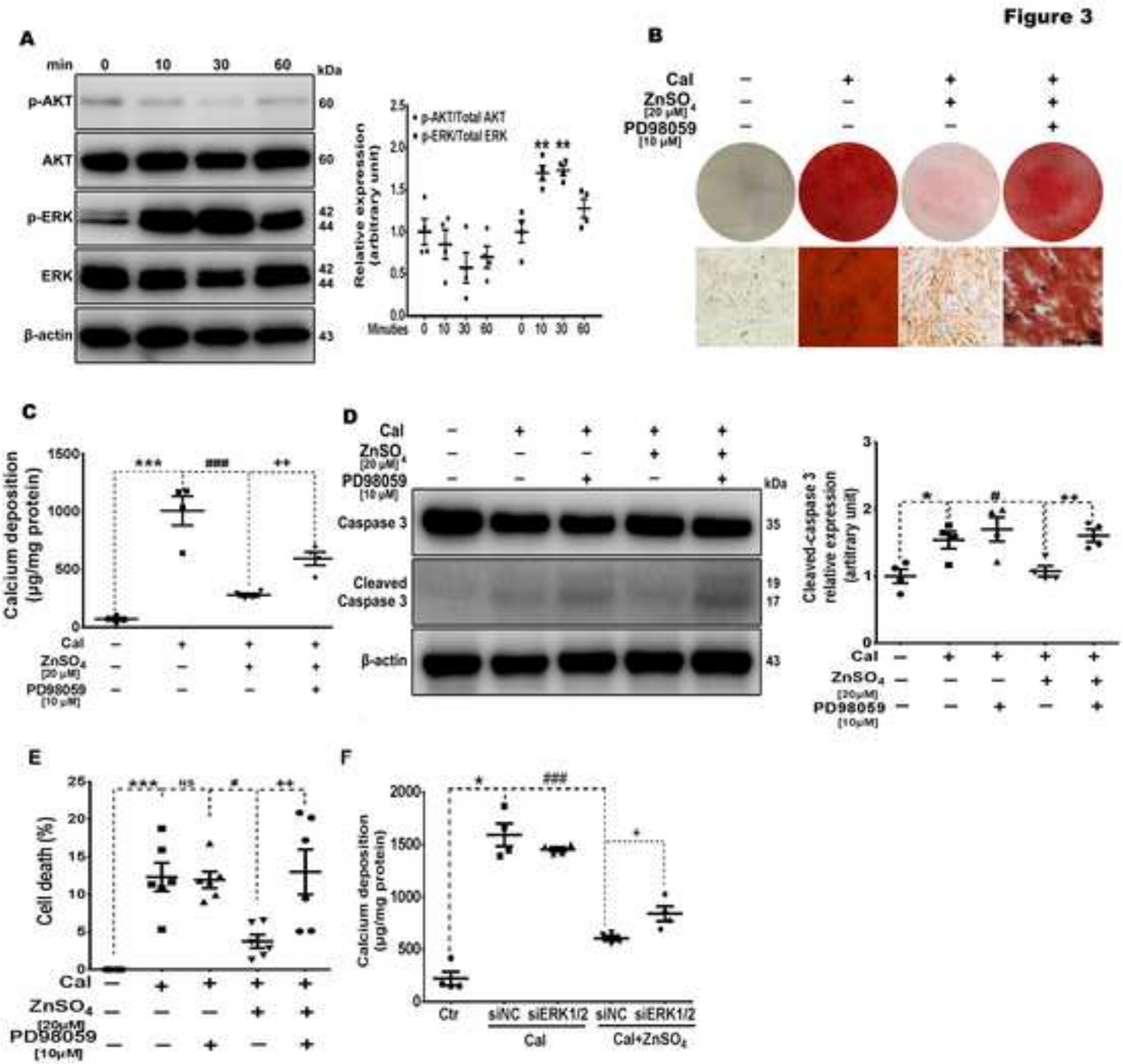

Figure 4

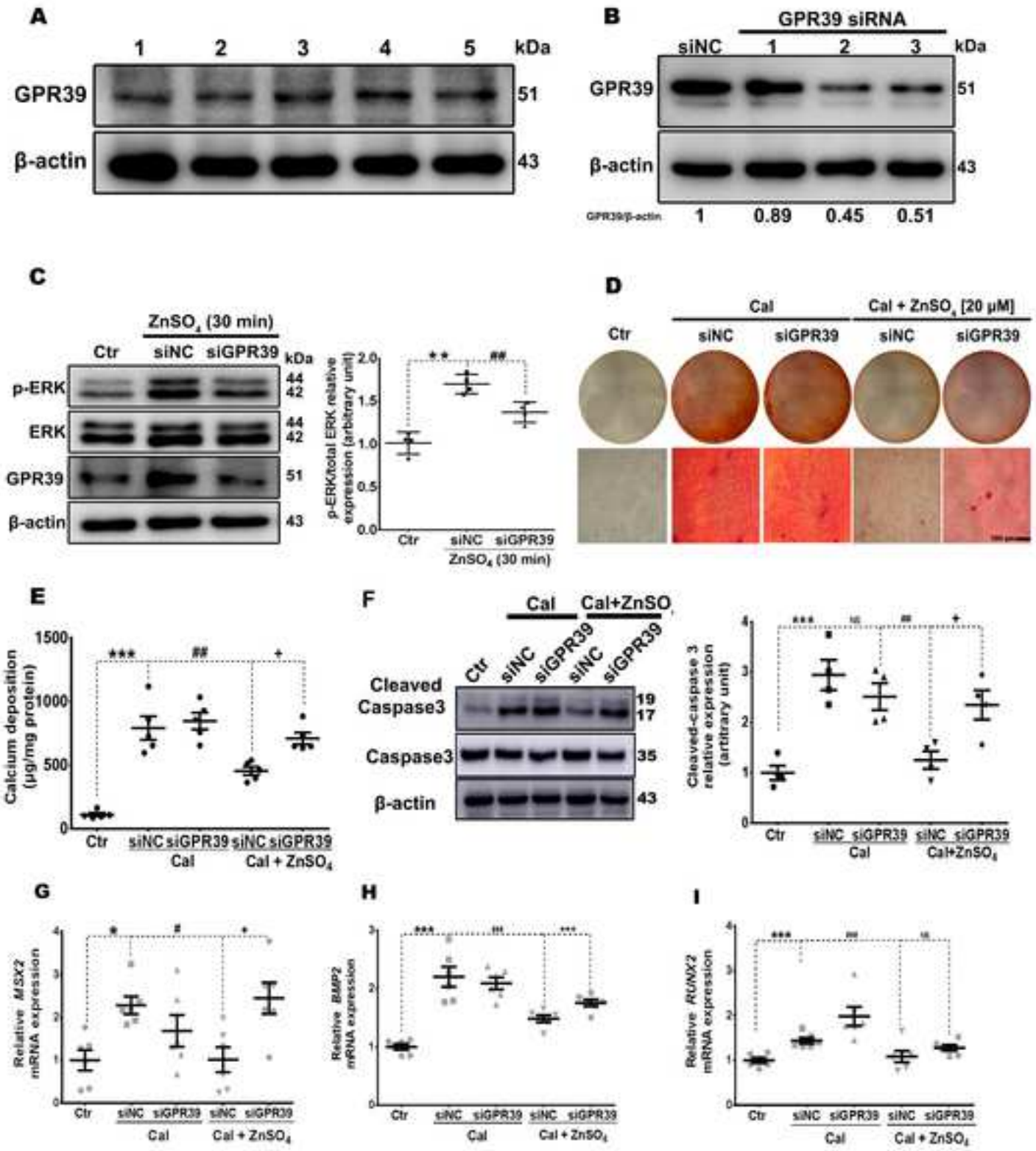
A
1 2 3 4 5 kDa
GPR39
β-actin
51
43
B
GPR39 siRNA
siNC 1 2 3 kDa
GPR39
β-actin
51
43
GPR39/β-actin 1 0.89 0.45 0.51
C
ZnSO4 (30 min)
Ctr siNC siGPR39 kDa
p-ERK
ERK
GPR39
β-actin
44
42
44
42
51
43
p-ERK/total ERK relative expression (arbitrary unit)
Ctr siNC siGPR39
ZnSO4 (30 min)
D
Cal
Cal + ZnSO4 [20 μM]
Ctr siNC siGPR39 siNC siGPR39
E
Calcium deposition (μg/mg protein)
Ctr siNC siGPR39 siNC siGPR39
Cal Cal + ZnSO4
F
Cal Cal+ZnSO4
Ctr siNC siGPR39 siNC siGPR39
Cleaved Caspase3
Caspase3
β-actin
19
17
35
43
Cleaved-caspase 3 relative expression (arbitrary unit)
Ctr siNC siGPR39 siNC siGPR39
Cal Cal+ZnSO4
G
Relative MSX2 mRNA expression
Ctr siNC siGPR39 siNC siGPR39
Cal Cal + ZnSO4
H
Relative BMP2 mRNA expression
Ctr siNC siGPR39 siNC siGPR39
Cal Cal + ZnSO4
I
Relative RUNX2 mRNA expression
Ctr siNC siGPR39 siNC siGPR39
Cal Cal + ZnSO4

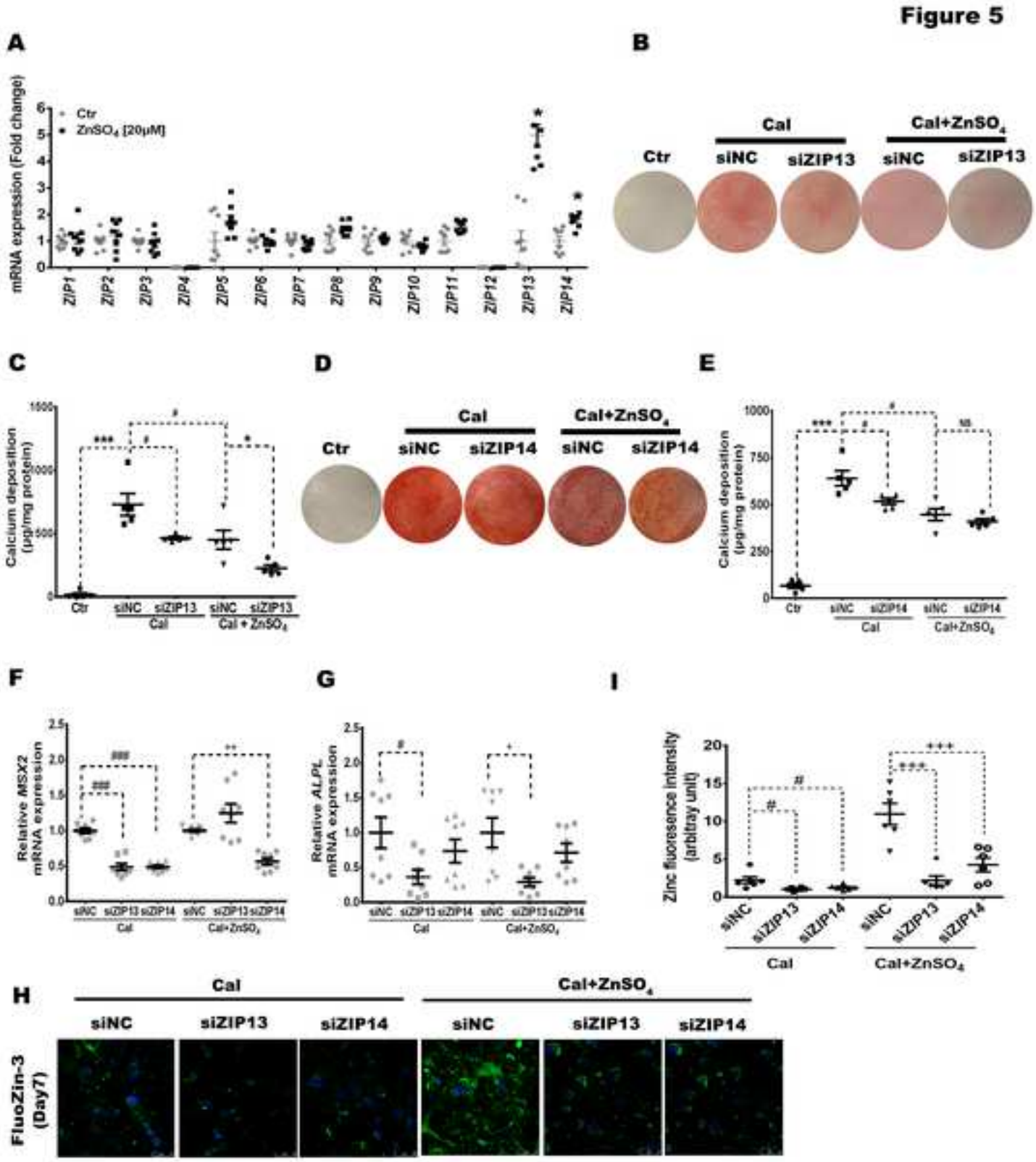

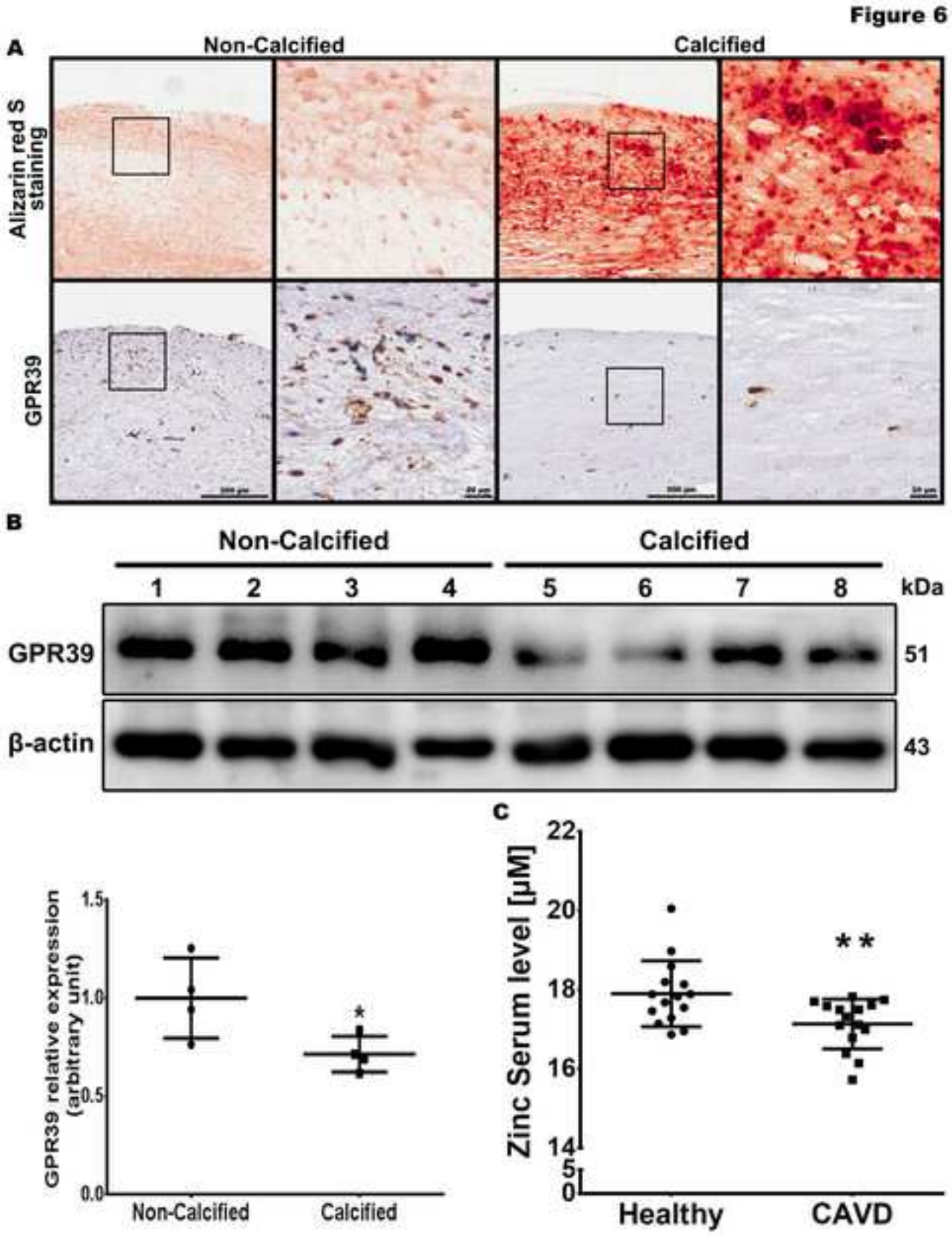
Figure 6
A
Non-Calcified
Calcified
Alizarin red S staining
GPR39
B
Non-Calcified
Calcified
1
2
3
4
5
6
7
8
kDa
GPR39
51
β-actin
43
GPR39 relative expression (arbitrary unit)
1.5
1.0
0.5
0.0
*
Non-Calcified
Calcified
C
Zinc Serum level [μM]
22
20
18
16
14
5
0
**
Healthy
CAVD

Figure 7

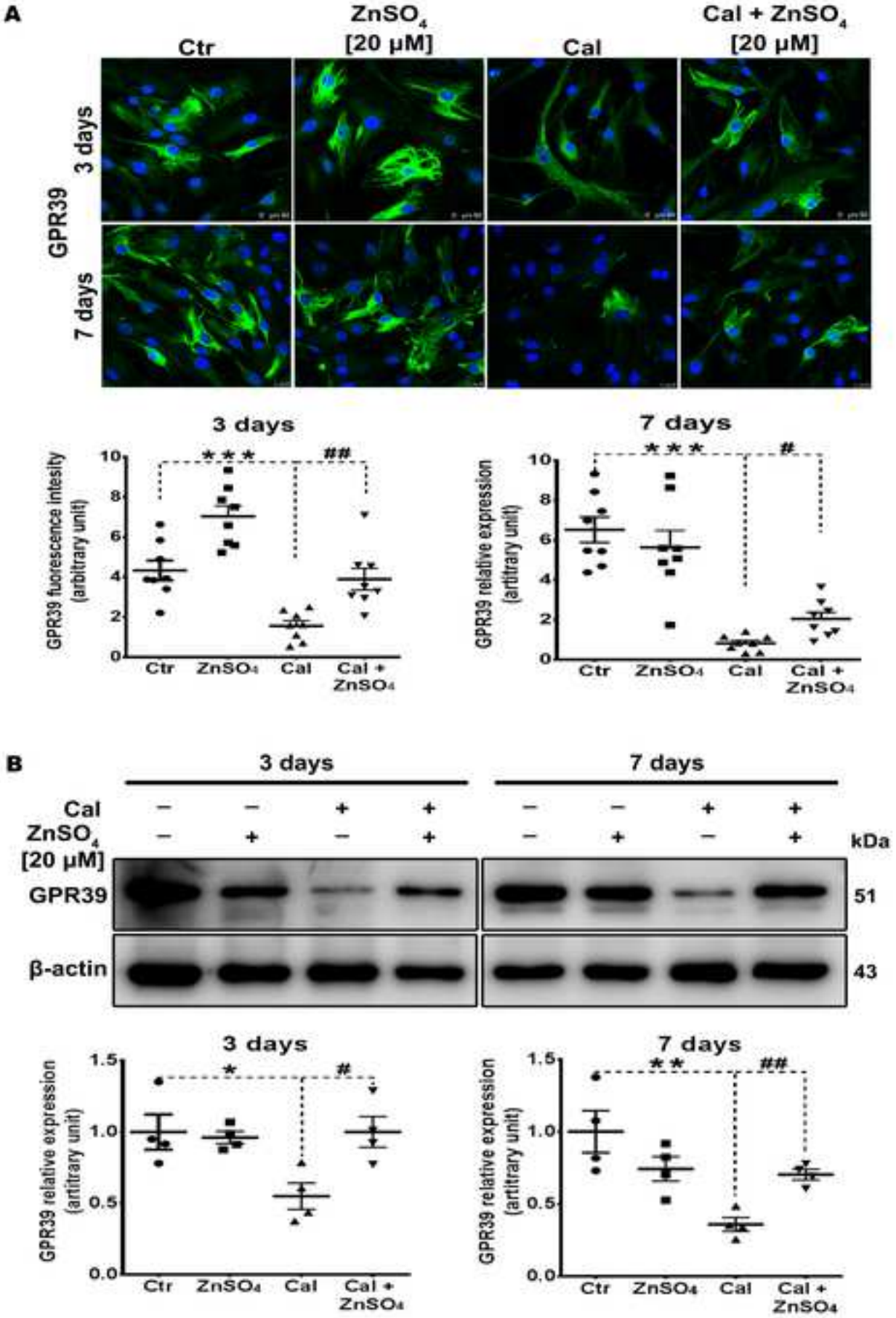

Graphical Abstract

Graphic abstract

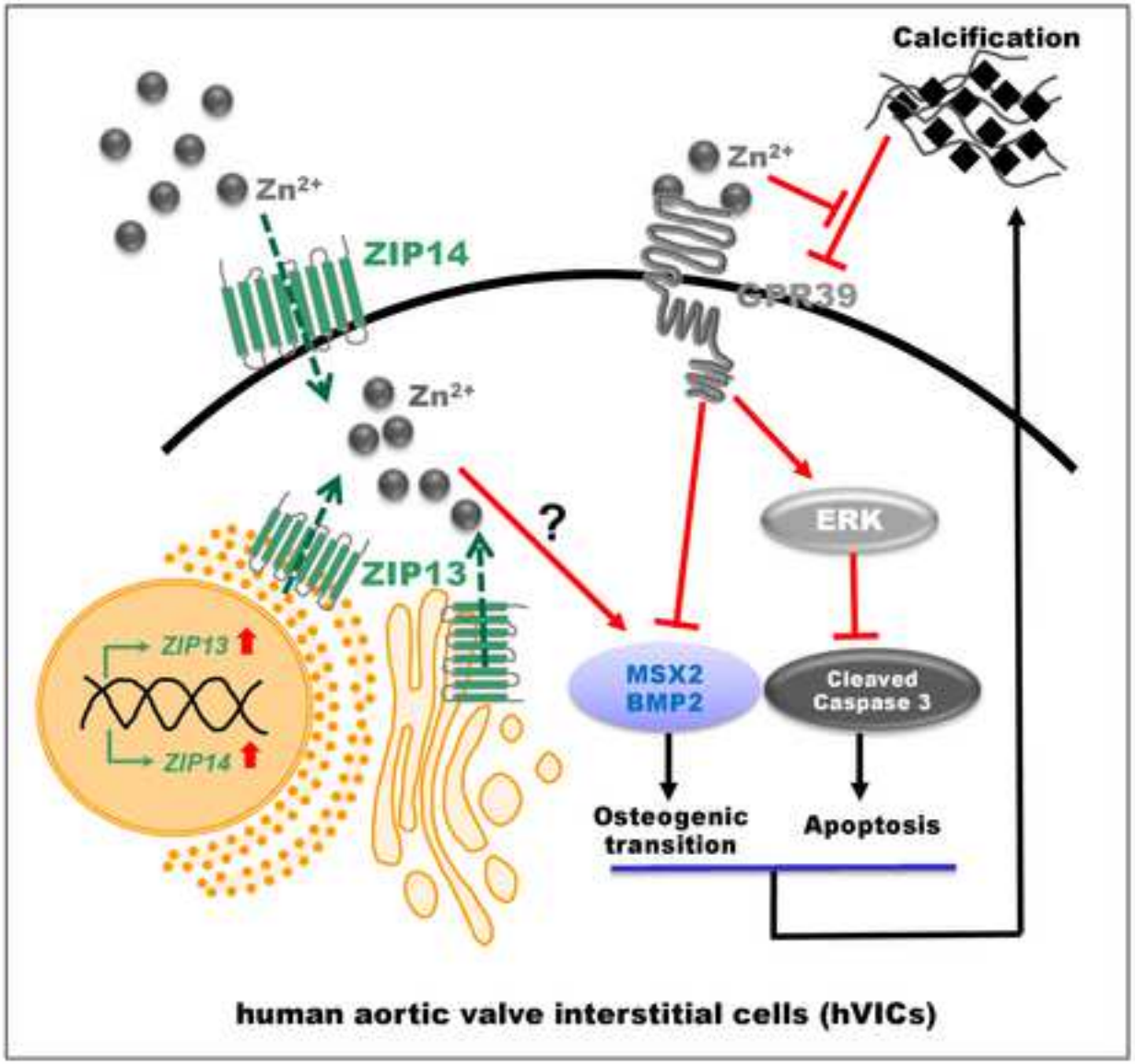

Zinc ameliorates human aortic valve calcification through GPR39 mediated ERK1/2 signaling pathway

Ziying Chen[1#], Flora Gordillo-Martinez[1#], Lei Jiang[2#], Pengcheng He[3], Wanzi Hong[3], Xuebiao Wei[3], Katherine A Staines[4], Vicky E. Macrae[5], Chunxiang Zhang[6], Danqing Yu[3*], Xiaodong Fu[1*], Dongxing Zhu[1*]

1. Guangzhou Institute of Cardiovascular Disease, Guangdong Key Laboratory of Vascular Diseases, State Key Laboratory of Respiratory Disease, the Second Affiliated Hospital, Guangzhou Medical University, Guangzhou, Guangdong, 510260, P.R.China.
2. Guangdong Geriatric Institute, Guangdong Provincial People's Hospital, Guangdong Academy of Medical Sciences, Guangzhou 510080, China.
3. Department of Cardiology, Guangdong Cardiovascular Institute, Guangdong Provincial People's Hospital, Guangdong Academy of Medical Sciences, Guangzhou 510080, China.
4. School of Applied Sciences, Edinburgh Napier University, Edinburgh, EH11 4BN, UK.
5. The Roslin Institute, RDSVS, Easter Bush Campus, University of Edinburgh, Midlothian, EH25 9RG, UK.
6. Department of Biomedical Engineering, School of Medicine, The University of Alabama at Birmingham Birmingham, AL 35233, USA.

Supplementary Figure I

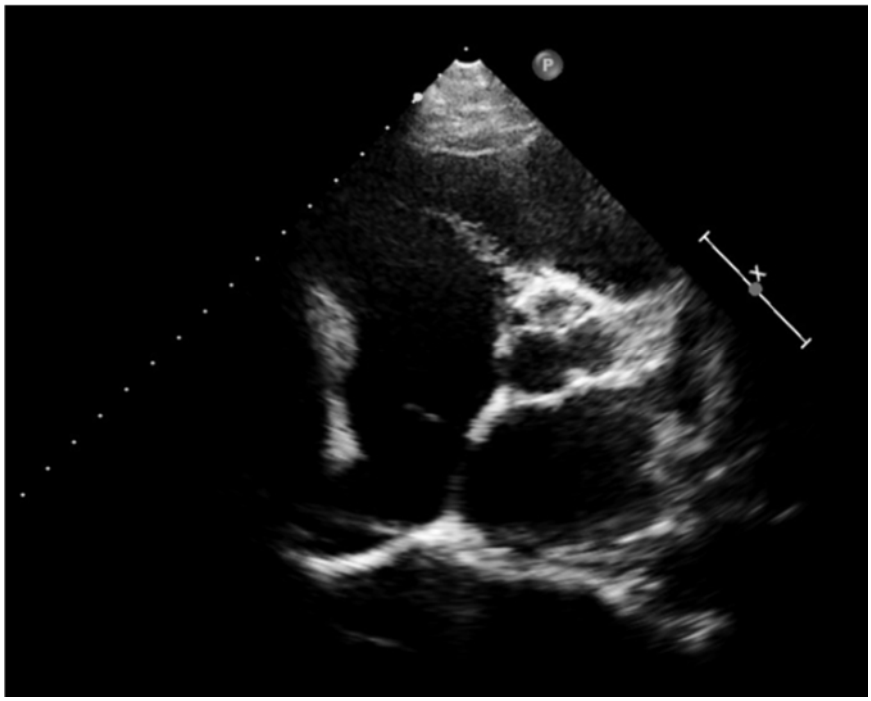

Supplementary Figure I. A representative still image of echocardiograms of a patient with CAVD.

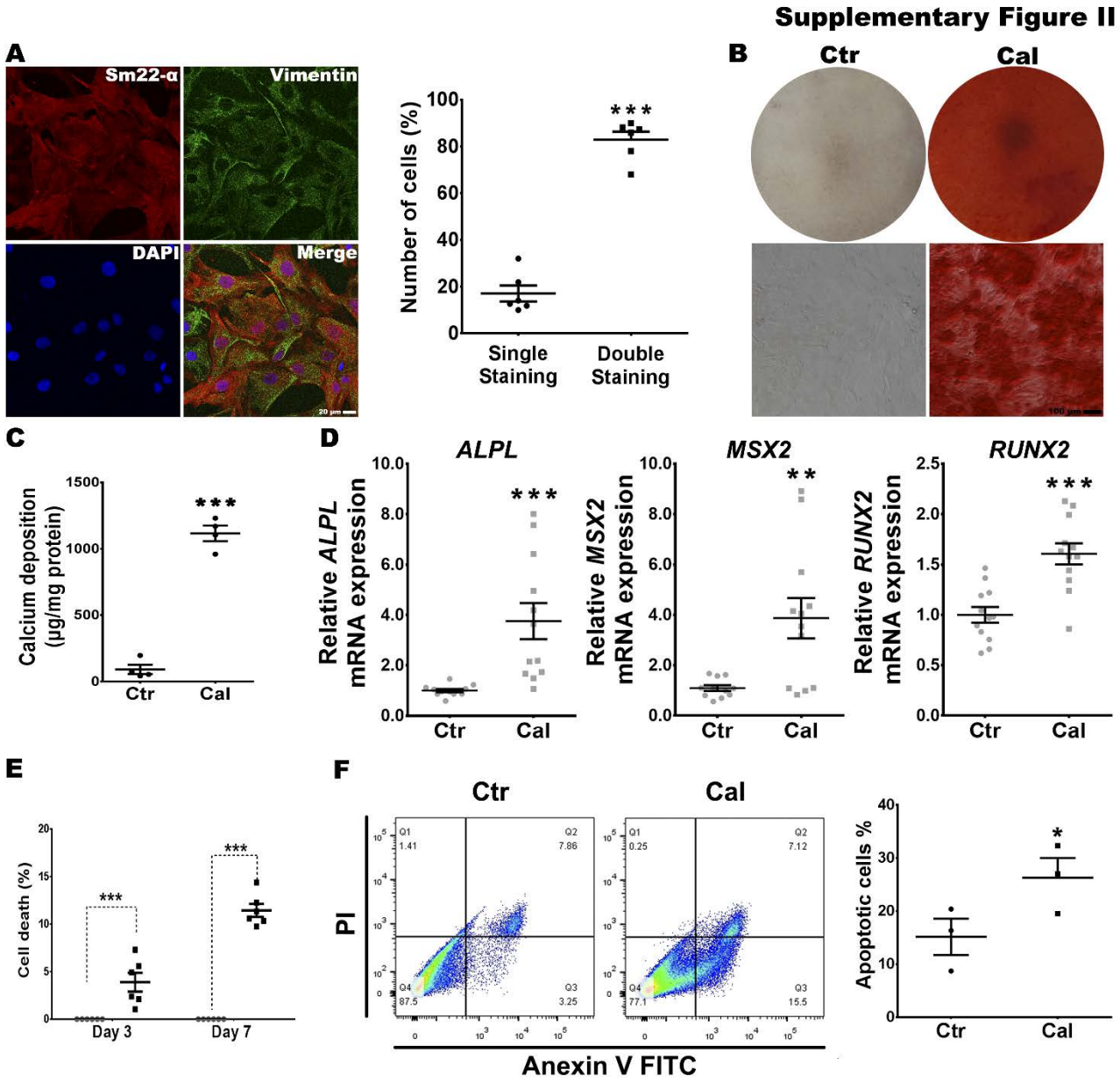

Supplementary Figure II. Validation of hVICs *in vitro* calcification model. hVICs were exposed to control (Ctr) or calcification media (Cal) for up to 7 days. **A.** Representative confocal images of vimentin and alpha 22-smooth muscle actin (Sm22-α) immunofluorescence staining (left panel) and quantitative analysis of percentage of cells expressing double valve interstitial cell markers (vimentin and Sm22-α) or single marker (right panel) (n=6). Scale bar 20 µm. **B**. Representative alizarin red S staining images at day 7 (n=3). Plate view (upper) and microscopic view (lower), scale bar 100 µm. **C.** Quantitative calcium assay at day 7 (n=4). **D.** Relative mRNA expression of ALPL, MSX2, and RUNX2 at day 2 (n=12), unpaired Student's t-test or Mann-Whitney test. **E.** Cell death at day 3 and day 7 (n=6). **F.** Flow cytometry analysis of Annexin V and Propidium Iodide (PI) staining (left panels) and quantification of the percentage of early apoptotic cells (Q3, right panel) at day 3 (n=3), unpaired Student's t-test. Results are presented as mean ± SEM.*$p < 0.05$, **$p < 0.01$, ***$p < 0.001$ compared to control.

Supplementary Figure III

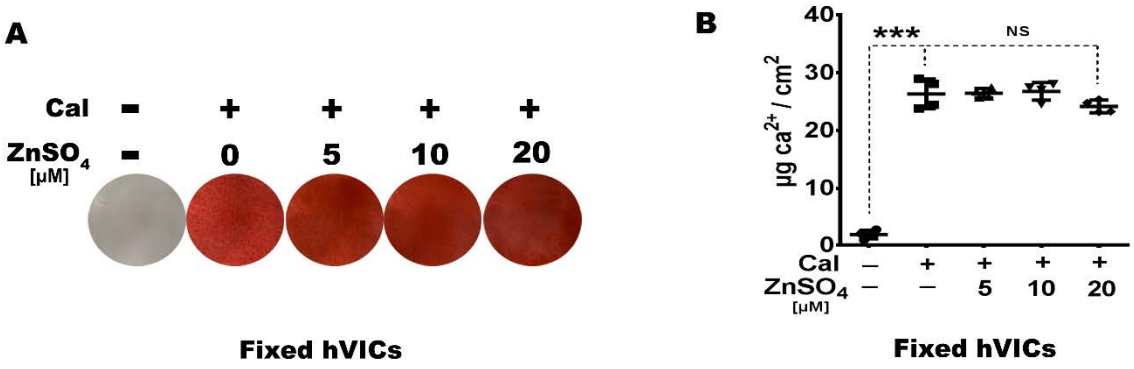

Supplementary Figure III. Zinc does not alter calcium deposition on fixed hVICs. hVICs were fixed with 4% PFA and then exposed to control (Ctr) or calcification media (Cal) without or with 20 µM of ZnSO4 treatment for 7 days. **A.** alizarin red staining. **B,** calcium quantitative assay (n=4). Results are presented as mean ± SEM. ANOVA by Bonferroni's test. ***p < 0.001 compared to control.

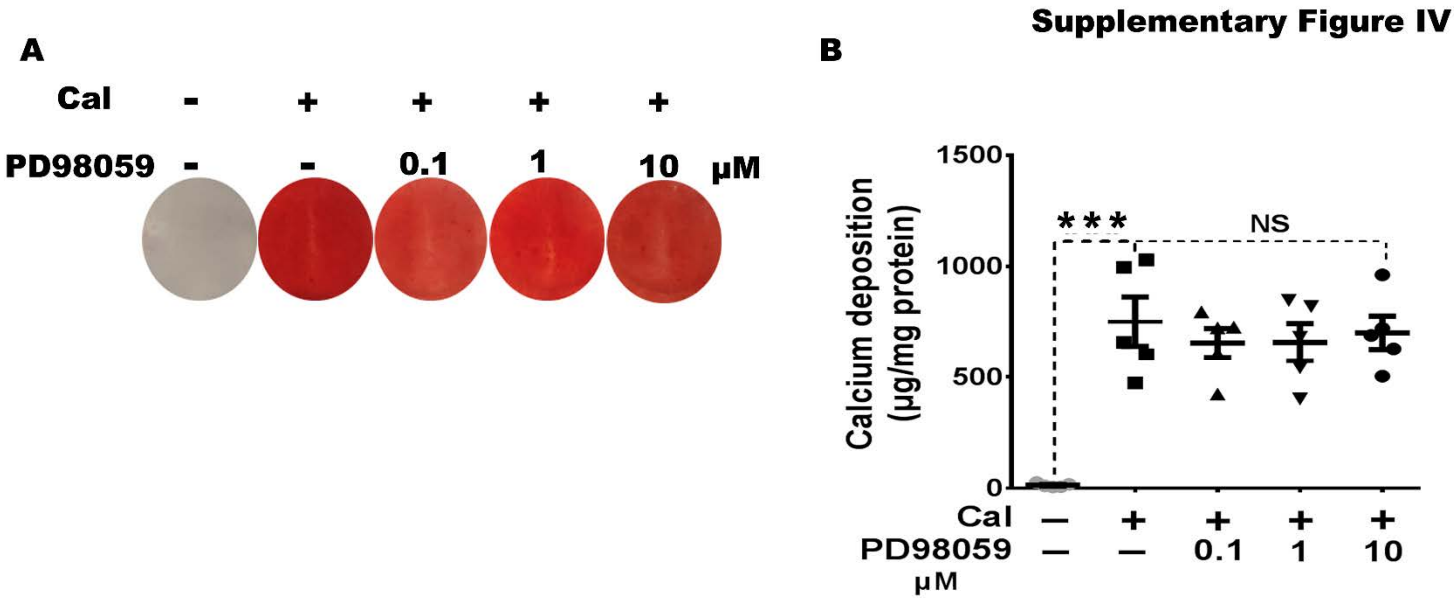

Supplementary Figure IV. ERK1/2 inhibitor PD98058 did not alter hVIC *in vitro* calcification. hVICs were exposed to control (Ctr) or calcification media (Cal) without or with 10 μM PD98059 for up to 7 days. **A.** Representative alizarin red S staining images at day 7 (n=3). **B.** Quantitative calcium assay at Day 7 (n=5).Results are presented as mean ± SEM. ANOVA by Bonferroni's test. ***$p < 0.001$ compared to control.

Supplementary Figure V

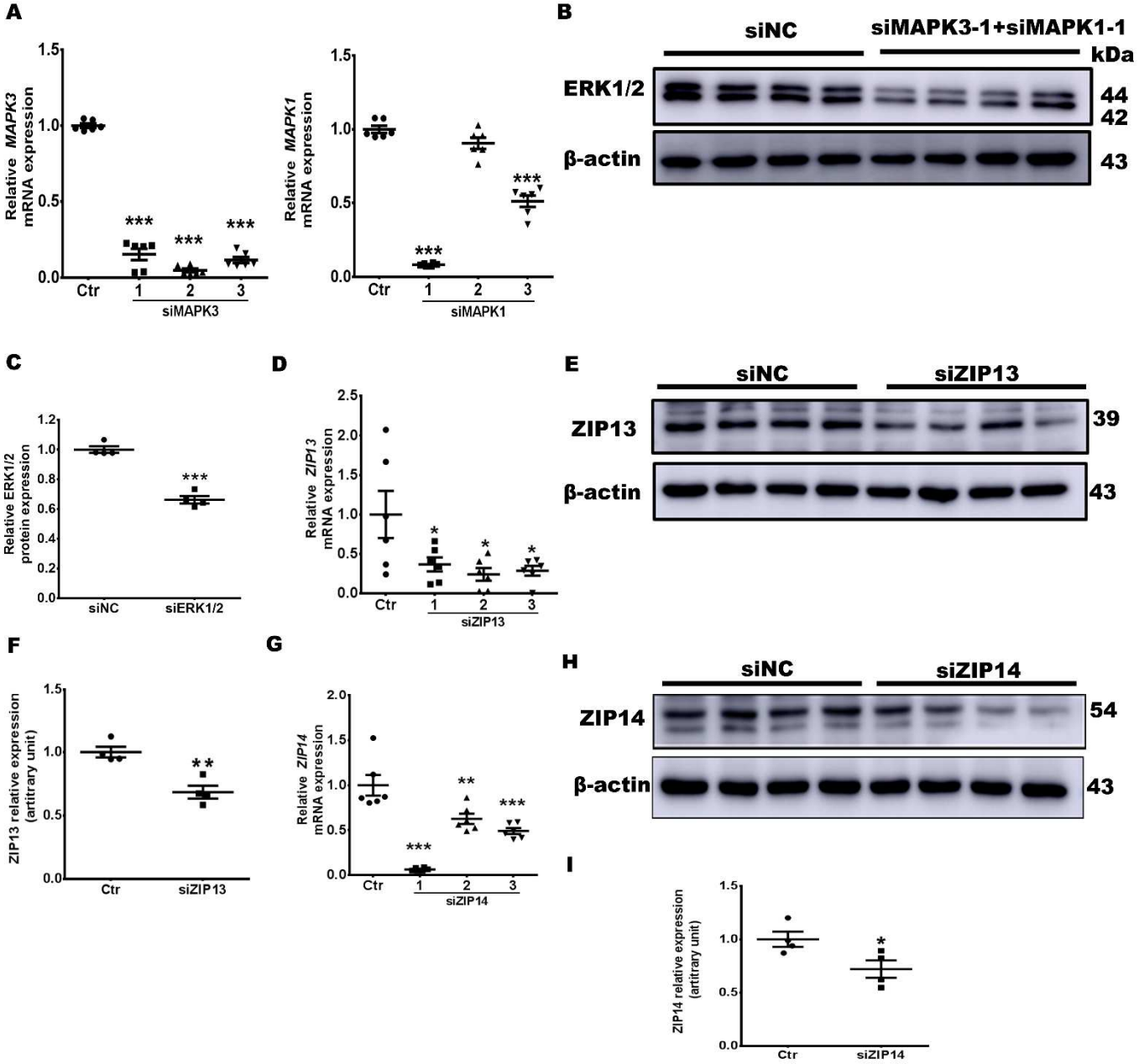

Supplementary Figure V. Knockdown efficiency of siERK1/2, siZIP13 and siZIP14. hVICs were transfected with siNC, siER1/2, siZIP13 or siZIP14 as indicated. **A.** Relative mRNA expression of ERK1 (*MAPK3) and* ERK2 *(MAPK1)* (n=6)*,* ANOVA by Bonferroni post-test. **B.** Western blotting images for ERK1/2 expression (n=4). **C.** Semi-quantitative analysis of expression of ERK1/2 (n=4), unpaired Student's t-test. **D.** Relative mRNA expression of ZIP13 (n=6)*,* ANOVA by Bonferroni post-test. **E.** Western blotting images for ZIP13 expression (n=4). **F.** Semi-quantitative analysis of expression of ZIP13 (n=4), unpaired Student's t-test. **G.** Relative mRNA expression of ZIP14 (n=6)*,* ANOVA by Bonferroni post-test. **H.** Western blotting images for ZIP14 expression (n=4). **I.** Semi-quantitative analysis of expression of ZIP14 (n=4), unpaired Student's t-test. Results are presented as mean ± SEM. ANOVA by Bonferroni's test. *p<0.05, **p<0.01, ***p < 0.001 compared to siNC.

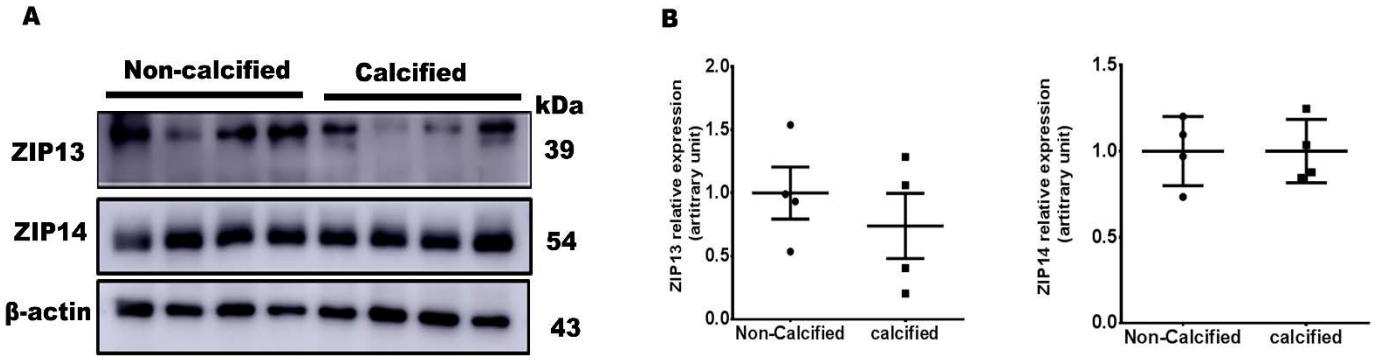

Supplementary Figure VI. ZIP13 and ZIP14 protein expression in human non-calcified and calcified aortic valves. A. Western blotting images for ZIP13 and ZIP14 expression (n=4). **B.** Semi-quantitative analysis of expression of ZIP13 and ZIP14 (n=4), unpaired Student's t-test. Results are presented as mean ± SEM.

Supplementary Table I. Clinical Characteristics of CAVD Patients for the isolation of hVICs.

Characteristics	CAVD (n=34)
Age, years	52.15±2.37
Male, %	74
Smoking, %	24
Hypertension, %	38
Diabetes mellitus, %	3
Bicuspid aortic valves, %	21
BMI, kg/m^2	22.81±0.57
Triglycerides, mmol/L	1.49±0.18
LDL, mmol/L	2.94±0.18
HDL, mmol/L	1.24±0.16
Cholesterol, μmol/L	4.53±0.24
Statins,%	24
Beta-blocker, %	50
ACEI/ARB, %	26

CAVD indicates calcific aortic valve disease; BMI, body mass index; LDL, low-density lipoprotein cholesterol; HDL, high-density lipoprotein cholesterol; ACEI/ARB, Angiotensin Converting Enzyme Inhibitors/Angiotensin Receptor Blockers. Values are mean±SEM when appropriate.

Supplementary Table II. Clinical Characteristics of Patients for the aortic valves studies.

Characteristics	Control (n=4)	CAVD (n=4)	P Value
Age, years	56±3.58	65±3.09	0.098
Male, %	100	100	1
Smoking, %	0	25	1
Hypertension, %	100	0	0.0286
Diabetes mellitus, %	0	0	1
Bicuspid aortic valves, %	0	0	1
BMI, kg/m2	23.19±1.2	24.63±1.88	0.5416
Triglycerides, mmol/L	1.27±0.32	1.05±0.08	0.5011
LDL, mmol/L	2.84±0.30	2.88±0.43	0.9495
HDL, mmol/L	0.84±0.13	1.23±0.18	0.1527
Cholesterol, μmol/L	4.40±0.34	4.66±0.54	0.693
Statins, %	25	0	1
Beta-blocker, %	75	50	1
ACEI/ARB, %	75	0	0.1429

CAVD indicates calcific aortic valve disease; BMI, body mass index; LDL, low-density lipoprotein cholesterol; HDL, high-density lipoprotein cholesterol; ACEI/ARB, Angiotensin Converting Enzyme Inhibitors/ Angiotensin Receptor Blockers. Values are mean±SEM when appropriate. P values determined by the Student t test or Fisher exact test.

Supplementary Table III. Clinical Characteristics of Patients for the Zinc Serum Level.

Characteristics	Control (n=15)	CAVD (n=15)	P Value
Age, years	69.47±1.34	73.4±1.64	0.0737
Male, %	53	100	0.2451
Smoking, %	NA	86	NA
Hypertension, %	NA	60	NA
Diabetes mellitus, %	NA	27	NA
Bicuspid aortic valves, %	NA	7	NA
BMI, kg/m^2	23.97±0.5	21.69±0.7	0.0131
Triglycerides, mmol/L	NA	1.33±0.16	NA
LDL, mmol/L	NA	2.92±0.20	NA
HDL, mmol/L	NA	1.26±0.34	NA
Cholesterol, μmol/L	NA	4.58±0.23	NA
Statins, %	NA	73	NA
Beta-blocker, %	NA	67	NA
Marked increase in echogenicity of aortic valves	0	15	<0.0001
LVEF, %	57.73±3.37	54.95±3.81	0.5903
AV, m/s	1.173±0.07	1.486±0.11	0.0186
AOD, cm	2.94±0.07	2.97±0.09	0.8076

CAVD indicates calcific aortic valve disease; BMI, body mass index; LDL, low-density lipoprotein cholesterol; HDL, high-density lipoprotein cholesterol; ACEI/ARB, Angiotensin Converting Enzyme Inhibitors/ Angiotensin Receptor Blockers; LVEF, left ventricular ejection fraction; AV, Aortic valve orifice velocity; AOD, Aortic diameter; Values are mean±SEM when appropriate. P values determined by the Student t test or Fisher exact test.

Supplementary Table IV

STROBE Statement—Checklist of items that should be included in reports of ***case-control studies***

	Item No	Recommendation	Page No
Title and abstract	1	(*a*) Indicate the study's design with a commonly used term in the title or the abstract	1
		(*b*) Provide in the abstract an informative and balanced summary of what was done and what was found	1
Introduction			
Background/rationale	2	Explain the scientific background and rationale for the investigation being reported	2-3
Objectives	3	State specific objectives, including any prespecified hypotheses	2-3
Methods			
Study design	4	Present key elements of study design early in the paper	3
Setting	5	Describe the setting, locations, and relevant dates, including periods of recruitment, exposure, follow-up, and data collection	3
Participants	6	(*a*) Give the eligibility criteria, and the sources and methods of case ascertainment and control selection. Give the rationale for the choice of cases and controls	3
		(*b*) For matched studies, give matching criteria and the number of controls per case	N/A
Variables	7	Clearly define all outcomes, exposures, predictors, potential confounders, and effect modifiers. Give diagnostic criteria, if applicable	3, Supplementary table III
Data sources/ measurement	8*	For each variable of interest, give sources of data and details of methods of assessment (measurement). Describe comparability of assessment methods if there is more than one group	3
Bias	9	Describe any efforts to address potential sources of bias	3
Study size	10	Explain how the study size was arrived at	3,10
Quantitative variables	11	Explain how quantitative variables were handled in the analyses. If applicable, describe which groupings were chosen and why	3,10, Supplementary Methods
Statistical methods	12	(*a*) Describe all statistical methods, including those used to control for confounding	6-7,10, Supplementary Methods
		(*b*) Describe any methods used to examine subgroups and interactions	N/A
		(*c*) Explain how missing data were addressed	3,10, Supplementary Methods
		(*d*) If applicable, explain how matching of cases and controls was addressed	3,10
		(*e*) Describe any sensitivity analyses	N/A
Results			
Participants	13*	(a) Report numbers of individuals at each stage of study—eg numbers potentially eligible, examined for eligibility, confirmed eligible, included in the study, completing follow-up, and analysed	3
		(b) Give reasons for non-participation at each stage	3
		(c) Consider use of a flow diagram	N/A

Descriptive data	14*	(a) Give characteristics of study participants (eg demographic, clinical, social) and information on exposures and potential confounders	Supplementary table III
		(b) Indicate number of participants with missing data for each variable of interest	3, Supplementary table III
Outcome data	15*	Report numbers in each exposure category, or summary measures of exposure	Supplementary table III

Main results	16	(*a*) Give unadjusted estimates and, if applicable, confounder-adjusted estimates and their precision (eg, 95% confidence interval). Make clear which confounders were adjusted for and why they were included	10, Supplementary table III, Figure 6C
		(*b*) Report category boundaries when continuous variables were categorized	10, Supplementary table III, Figure 6C
		(*c*) If relevant, consider translating estimates of relative risk into absolute risk for a meaningful time period	N/A
Other analyses	17	Report other analyses done—eg analyses of subgroups and interactions, and sensitivity analyses	N/A
Discussion			
Key results	18	Summarise key results with reference to study objectives	10-14
Limitations	19	Discuss limitations of the study, taking into account sources of potential bias or imprecision. Discuss both direction and magnitude of any potential bias	13-14
Interpretation	20	Give a cautious overall interpretation of results considering objectives, limitations, multiplicity of analyses, results from similar studies, and other relevant evidence	10-14
Generalisability	21	Discuss the generalisability (external validity) of the study results	10-14
Other information			
Funding	22	Give the source of funding and the role of the funders for the present study and, if applicable, for the original study on which the present article is based	14

*Give information separately for cases and controls.

Note: An Explanation and Elaboration article discusses each checklist item and gives methodological background and published examples of transparent reporting. The STROBE checklist is best used in conjunction with this article (freely available on the Web sites of PLoS Medicine at http://www.plosmedicine.org/, Annals of Internal Medicine at http://www.annals.org/, and Epidemiology at http://www.epidem.com/). Information on the STROBE Initiative is available at http://www.strobe-statement.org.

Supplementary Table V. The qPCR primer sequences for target genes

Gene	Forward primer (5'-3')	Reverse primer (5'-3')
RUNX2	GCCTTCCACTCTCAGTAAGAAGA	GCCTGGGGTCTGAAAAAGGG
ALPL	ACTGGTACTCAGACAACGAGAT	ACGTCAATGTCCCTGATGTTATG
MSX2	TGGATGCAGGAACCCGG	AGGGCTCATATGTCTTGGCG
BMP2	TTCGGCCTGAAACAGAGACC	CCTGAGTGCCTGCGATACAG
GAPDH	GAGTCAACGGATTTGGTCGT	GACAAGCTTCCCGTTCTCAG
ZIP1	ACTACCTGGCTGCCATAGATG	GCCCTGACTGCTCCTTGTAAG
ZIP2	TCACAGATTCAGAAGTTCATGGT	GCTCTCCATAGGGATACTCCA
ZIP3	CTCGGCCACATCAGCAC	TTGAAGGTCTCCAGGTCGAT
ZIP4	AAGATGGCCTGCGTAGATA	TGCTGCTGGAACACAAAG
ZIP5	GGGGCTGTCAGTGCTCGGAG	TCCGGATCCAAGTTGCGTGTT
ZIP6	CAACTATCTCTGTCCAGCCATC	CCACCAACCCAGGCTATTT
ZIP7	CTCTACTTCAGATCTTGCTCAGTT	TGGTGAGAATGAGGTTCAAGAG
ZIP8	TGCTACCCAAATAACCAGCTCC	ACAGGAATCCATATCCCCAAACT
ZIP9	TCTCTGGCTATGTTGGTGGGA	CCAGCACCCAAAACAGTCAC
ZIP10	ACACCAGATTCTGACTGGCTT	TAGGAGGGGATTCTTGTTGGC
ZIP11	TGCTGGGGACCTTCTTCAC	GCCAAGACTTCCATCTAAGATCC
ZIP12	TTTCCTGGGATCAGACCTGCT	GTTGGTCCTTGGGTAAGTGGC
ZIP13	TCCTGGGTTCCCTCATGGT	AGATGCAGAAACACATTGCCC
ZIP14	GGCTGCTGCTCTACTTCATAG	TCCAGAGGGTTGAAACCAAAT
MAPK1	TACACCAACCTCTCGTACATCG	CATGTCTGAAGCGCAGTAAGATT
MAPK3	CTACACGCAGTTGCAGTACAT	CAGCAGGATCTGGATCTCCC
TNFα	GAGGCCAAGCCCTGGTATG	CGGGCCGATTGATCTCAGC
TGFβ1	CAATTCCTGGCGATACCTCAG	GCACAACTCCGGTGACATCAA

Supplementary Table VI. siRNA sequences for gene silencing

siRNA	Sequence (5'-3')
GPR39 siRNA 1	AGUGACUGCUCCCAAAUCA
GPR39 siRNA 2	GACAGACCACAUGGUGAGU
GPR39 siRNA 3	AUGCCCAUGGAGUUCUACA
MAPK1 siRNA 1	GAACATCATTGGAATCAAT
MAPK1 siRNA 2	GCTACACCAACCTCTCGTA
MAPK1 siRNA 3	GCACCAACCATCGAGCAAA
MAPK3 siRNA 1	CCTCCAACCTGCTCATCAA
MAPK3 siRNA 2	GACCGGATGTTAACCTTTA
MAPK3 siRNA 3	GCTACACGCAGTTGCAGTA
ZIP13 siRNA 1	GCTTCCTTGTGAGCAAGAA
ZIP13 siRNA 2	CTGACCTCTTGGAAGAAGA
ZIP13 siRNA 3	CTGGCCAACACCATCGATA
ZIP14 siRNA1	GGAGGAATGTTCTTGTATA
ZIP14 siRNA2	GGTGTCCGCTAACTCTGATA
ZIP14 siRNA3	GGAGTTCCCACATGAGCTA

Supplementary Methods

All statistical testing was 2-sided, with $P < 0.05$ considered significant. Analyses were performed using IBM SPSS Statistics 19.0 (IBM Corporation, Chicago, USA). The comparison of the baseline variables of interest were performed according to the patients with CAVD or not. Continuous variables, such as age, Zn and BMI, were denoted as mean ± standard deviation, and student's t test was conducted to compare the variables. Category variables, such as sex, were denoted as number (proportions) of female, and χ^2 test was conducted to compare the variables. **Table 1**showed that there is a significant lower Zn concentration (17.1±0.6 vs 17.9 ± 0.8 μmol/L, P=0.014) and lower BMI (21.7 ± 2.7 vs 23.9 ± 1.9 kg/m^2, P=0.013) in CAVD group. There is no significant difference of sex and age between the two groups.

Table 1 baseline characteristics of different groups

Variables	CAVD (n =15)	non-CAVD (n =15)	P value
Age, Mean (SD), y	73.4 (6.4)	69.5 (5.2)	0.074
Female, No. (%)	3 (20)	7 (47)	0.13
Zn, mean (SD), μ mol/L	17.1 (0.6)	17.9 (0.8)	0.014
BMI, mean (SD), kg/m^2	21.7(2.7)	23.9 (1.9)	0.013

Table 2 showed the univariate and multivariate analyses of the variables predicting CAVD. The increasing Zn and BMI showed to be a significant protect factor of CAVD from the univariate analyses. After adjusting all the 4 variables of baseline, only the increasing BMI is the independent protective factor with a statistical significance (OR=0.598; C.I.: 0.371~0.966; P=0.035). There is an apparent trend in the final analyses to show the relationship between increasing Zn and CAVD

(OR=0.128; C.I.: 0.015~1.090; P=0.060). We believe that this negative result attribute to the small participates number.

Table 2 univariable and multivariable analysis

	Univariable analysis			Multivariable analysis		
	OR	95% C.I.	P	OR	95% C.I.	P
Age increase 1	1.132	[0.983~1.303]	0.084	1.111	[0.896~1.378]	0.339
Male	3.500	[0.692~17.714]	0.130	3.740	[0.394~35.482]	0.251
Zn increase 1	0.148	[0.026~0.826]	0.029	0.128	[0.015~1.090]	0.060
BMI increase 1	0.653	[0.449~0.950]	0.026	0.598	[0.371~0.966]	0.035

Furthermore, considering that there is no difference in the baseline and univariate analysis in age and sex and only 15 patients were diagnosed with CAVD, it is rational to include no more than 2 variables in the final multivariate analyses according to the statistical rule: the events per variable should be 10 or more. We performed a forward stepwise multivariate logistic analysis (likelihood ratio) to get a more convincible result. Only Zn and BMI were included in the final model (**Table 3**). From this result, increasing Zn was proved to be a significant protective factor of CAVD after adjusted the BMI (OR=0.135; C.I.: 0.022~0.815; P=0.029).

Table 3 univariable and multivariable analysis of forward stepwise logistic analysis

	Univariable analysis			Multivariable analysis		
	OR	95% C.I.	P	OR	95% C.I.	P
Age increase 1	1.132	[0.983~1.303]	0.084			
Male	3.500	[0.692~17.714]	0.130			
Zn increase 1	0.148	[0.026~0.826]	0.029	0.135	[0.022~0.815]	0.029
BMI increase 1	0.653	[0.449~0.950]	0.026	0.603	[0.377~0.966]	0.035

Figure 1

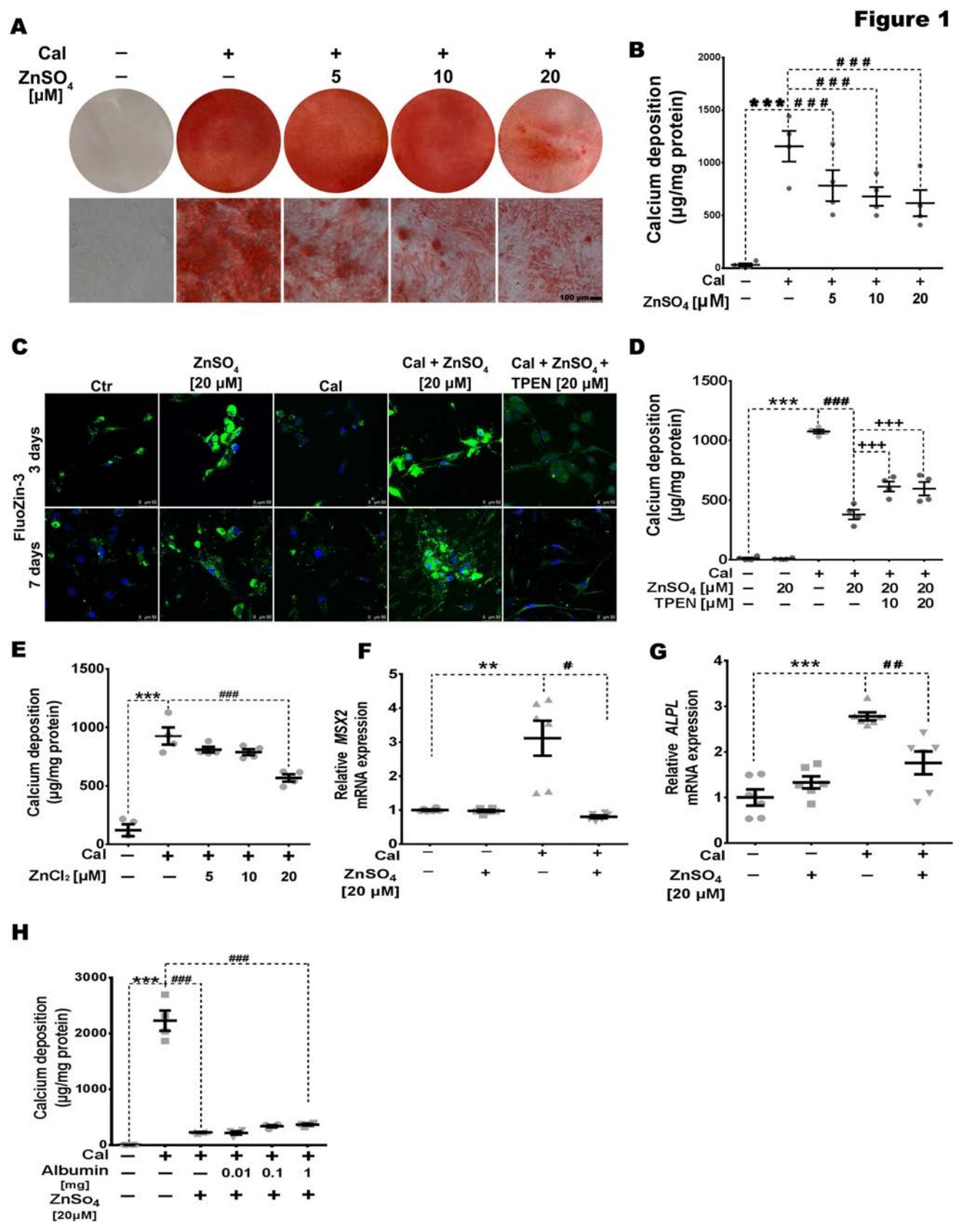
A
Cal
ZnSO4 [μM]
100 μm
B
Calcium deposition (μg/mg protein)
ZnSO4 [μM]
C
Ctr
ZnSO4 [20 μM]
Cal
Cal + ZnSO4 [20 μM]
Cal + ZnSO4 + TPEN [20 μM]
FluoZin-3
3 days
7 days
D
Calcium deposition (μg/mg protein)
ZnSO4 [μM]
TPEN [μM]
E
Calcium deposition (μg/mg protein)
ZnCl2 [μM]
F
Relative MSX2 mRNA expression
ZnSO4 [20 μM]
G
Relative ALPL mRNA expression
ZnSO4 [20 μM]
H
Calcium deposition (μg/mg protein)
Albumin [mg]
ZnSO4 [20μM]

Figure 2

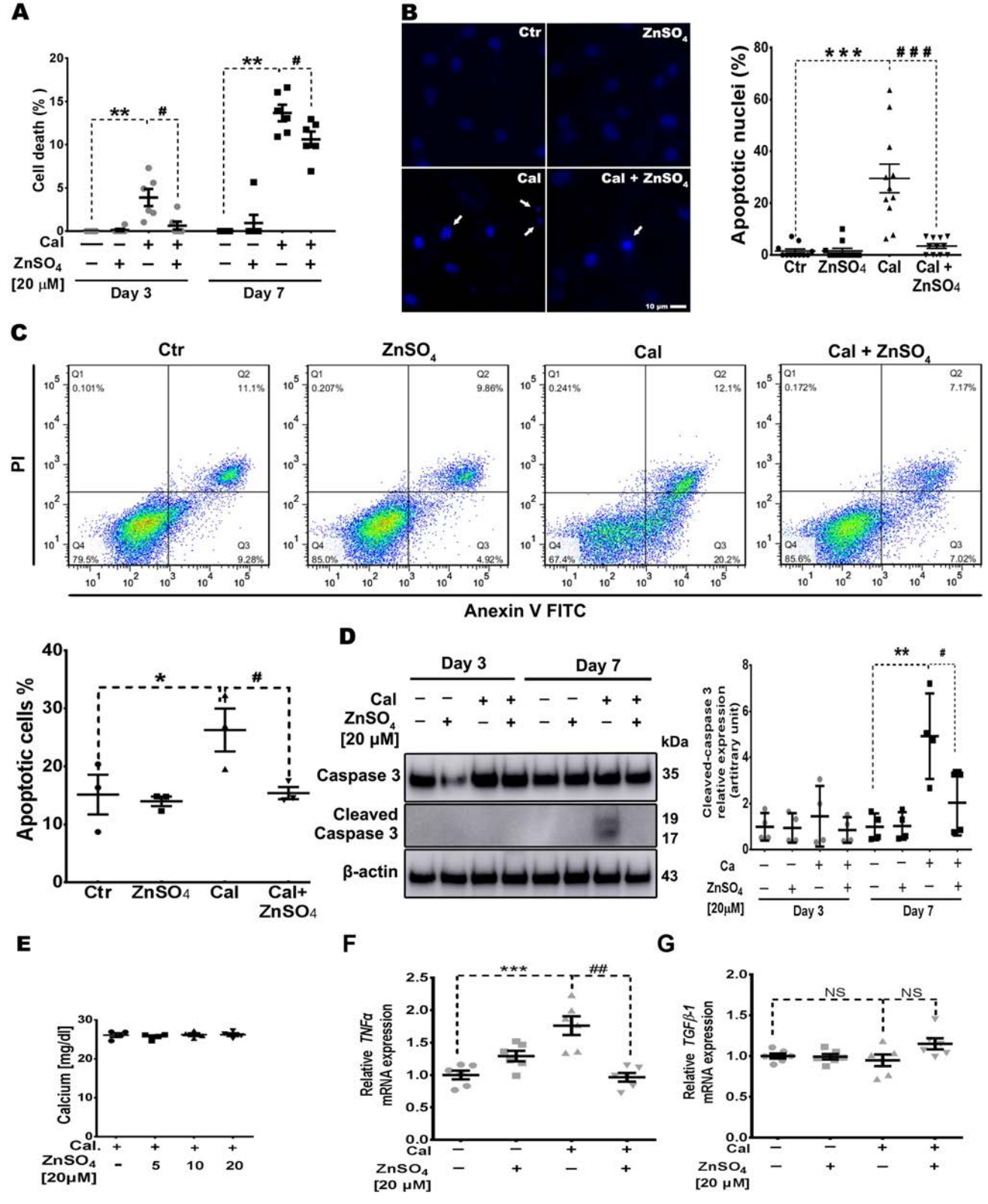
A
Cell death (%)
Cal
ZnSO4
[20 μM]
Day 3
Day 7
B
Ctr
ZnSO4
Cal
Cal + ZnSO4
10 μm
Apoptotic nuclei (%)
Ctr
ZnSO4
Cal
Cal + ZnSO4
C
Ctr
ZnSO4
Cal
Cal + ZnSO4
PI
Anexin V FITC
Q1 0.101%
Q2 11.1%
Q4 79.5%
Q3 9.28%
Q1 0.207%
Q2 9.86%
Q4 85.0%
Q3 4.92%
Q1 0.241%
Q2 12.1%
Q4 67.4%
Q3 20.2%
Q1 0.172%
Q2 7.17%
Q4 85.6%
Q3 7.02%
Apoptotic cells %
Ctr
ZnSO4
Cal
Cal+ ZnSO4
D
Day 3
Day 7
Cal
ZnSO4
[20 μM]
kDa
Caspase 3
35
Cleaved Caspase 3
19
17
β-actin
43
Cleaved-caspase 3 relative expression (artitrary unit)
Ca
ZnSO4
[20μM]
Day 3
Day 7
E
Calcium [mg/dl]
Cal.
ZnSO4
[20μM]
5
10
20
F
Relative TNFα mRNA expression
Cal
ZnSO4
[20 μM]
G
Relative TGFβ-1 mRNA expression
NS
NS
Cal
ZnSO4
[20 μM]

Figure 3

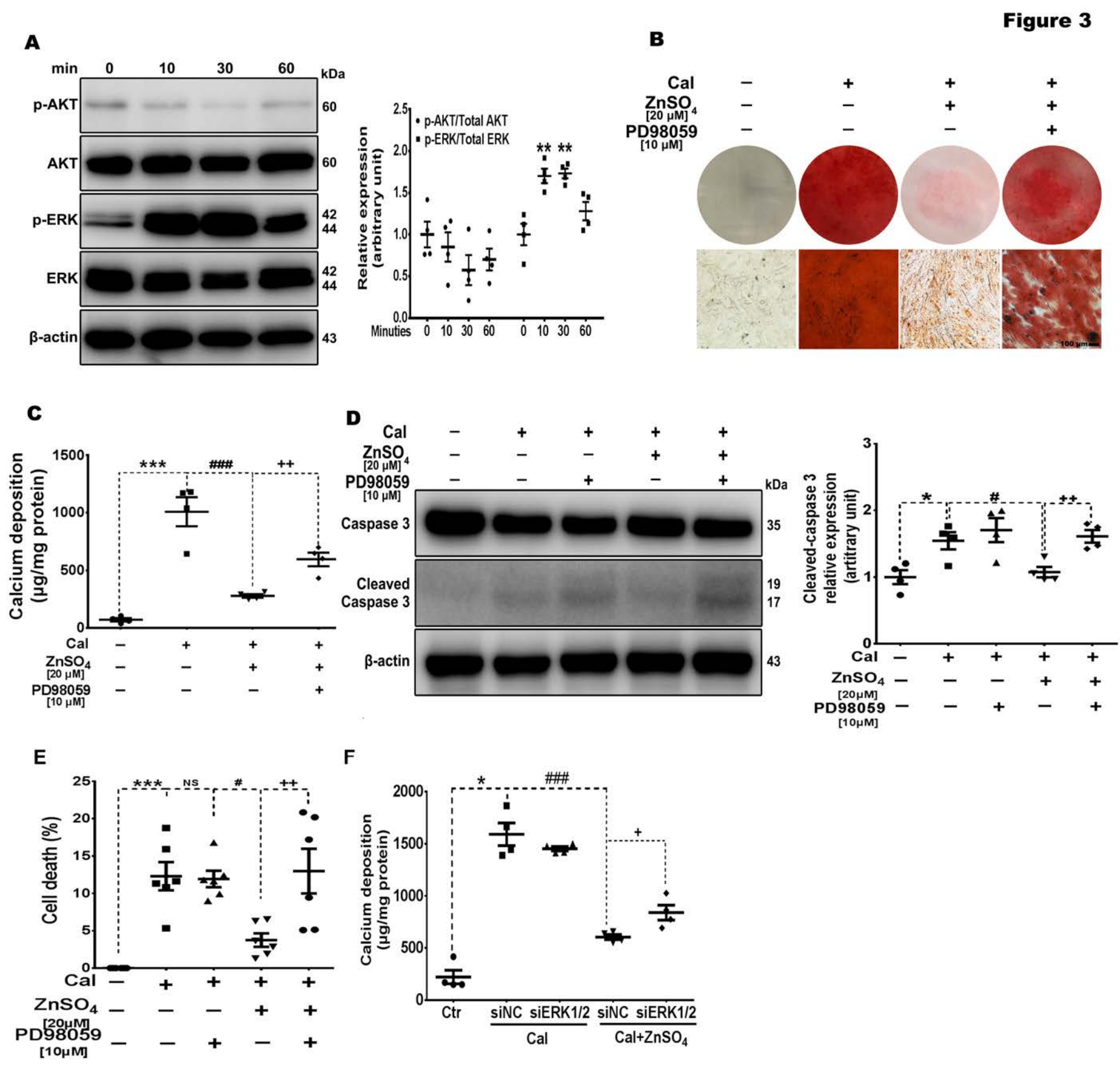
A
min 0 10 30 60 kDa
p-AKT 60
AKT 60
p-ERK 42 44
ERK 42 44
β-actin 43
p-AKT/Total AKT
p-ERK/Total ERK
Relative expression (arbitrary unit)
Minuties 0 10 30 60 0 10 30 60
B
Cal
ZnSO4 [20 μM]
PD98059 [10 μM]
100 μm
C
Calcium deposition (μg/mg protein)
Cal
ZnSO4 [20 μM]
PD98059 [10 μM]
D
Caspase 3 35
Cleaved Caspase 3 19 17
β-actin 43
Cleaved-caspase 3 relative expression (artitrary unit)
E
Cell death (%)
F
Calcium deposition (μg/mg protein)
Ctr
siNC siERK1/2
Cal
Cal+ZnSO4

Figure 4

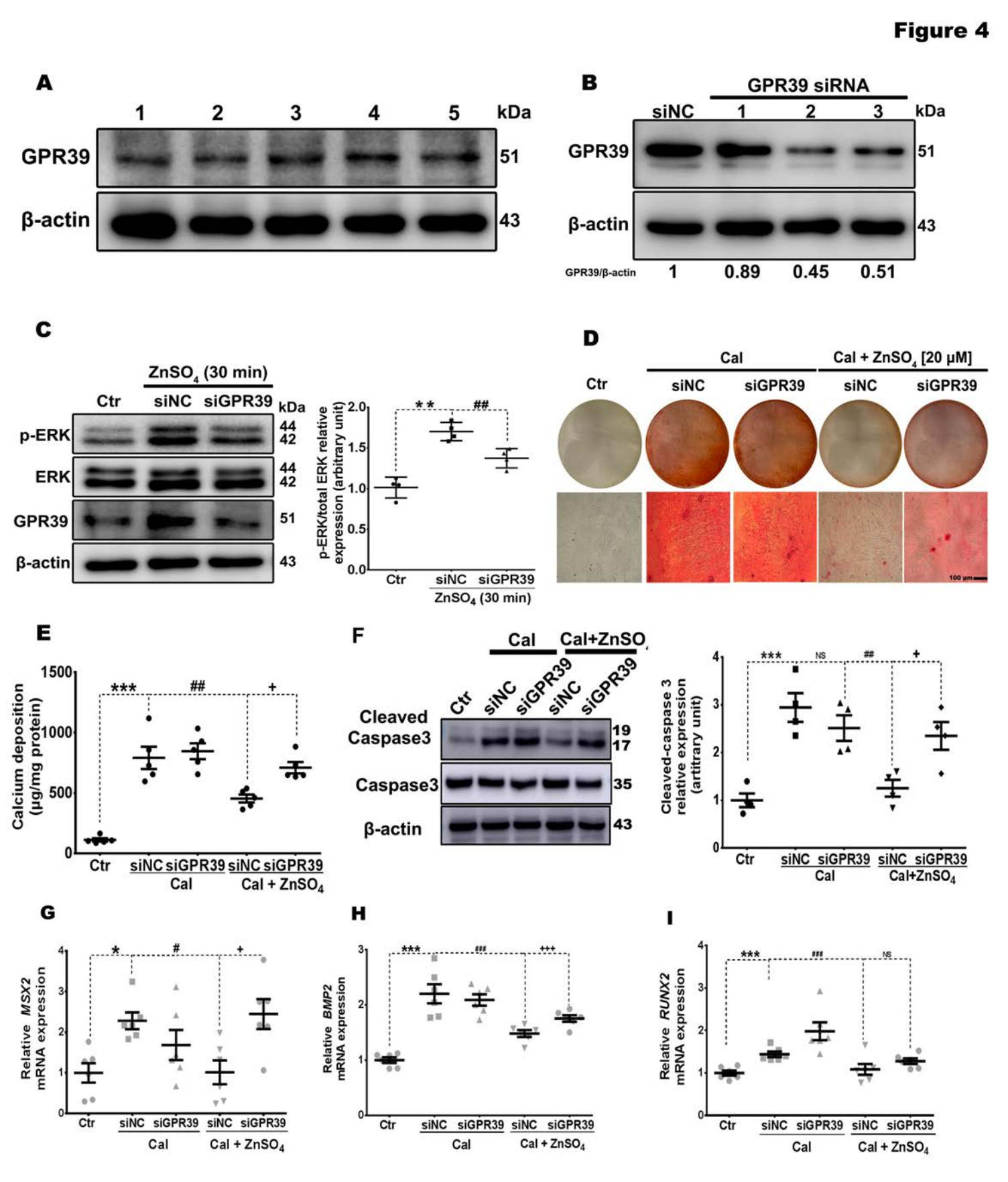
A
1 2 3 4 5 kDa
GPR39
β-actin
51
43
B
GPR39 siRNA
siNC 1 2 3 kDa
GPR39
β-actin
51
43
GPR39/β-actin 1 0.89 0.45 0.51
C
ZnSO4 (30 min)
Ctr siNC siGPR39 kDa
p-ERK
ERK
GPR39
β-actin
44
42
44
42
51
43
p-ERK/total ERK relative expression (arbitrary unit)
Ctr siNC siGPR39
ZnSO4 (30 min)
D
Cal
Cal + ZnSO4 [20 μM]
Ctr siNC siGPR39 siNC siGPR39
100 μm
E
Calcium deposition (μg/mg protein)
Ctr siNC siGPR39 siNC siGPR39
Cal Cal + ZnSO4
F
Cal Cal+ZnSO4
Ctr siNC siGPR39 siNC siGPR39
Cleaved Caspase3
Caspase3
β-actin
19
17
35
43
Cleaved-caspase 3 relative expression (arbitrary unit)
Ctr siNC siGPR39 siNC siGPR39
Cal Cal+ZnSO4
G
Relative MSX2 mRNA expression
Ctr siNC siGPR39 siNC siGPR39
Cal Cal + ZnSO4
H
Relative BMP2 mRNA expression
Ctr siNC siGPR39 siNC siGPR39
Cal Cal + ZnSO4
I
Relative RUNX2 mRNA expression
Ctr siNC siGPR39 siNC siGPR39
Cal Cal + ZnSO4

Figure 5

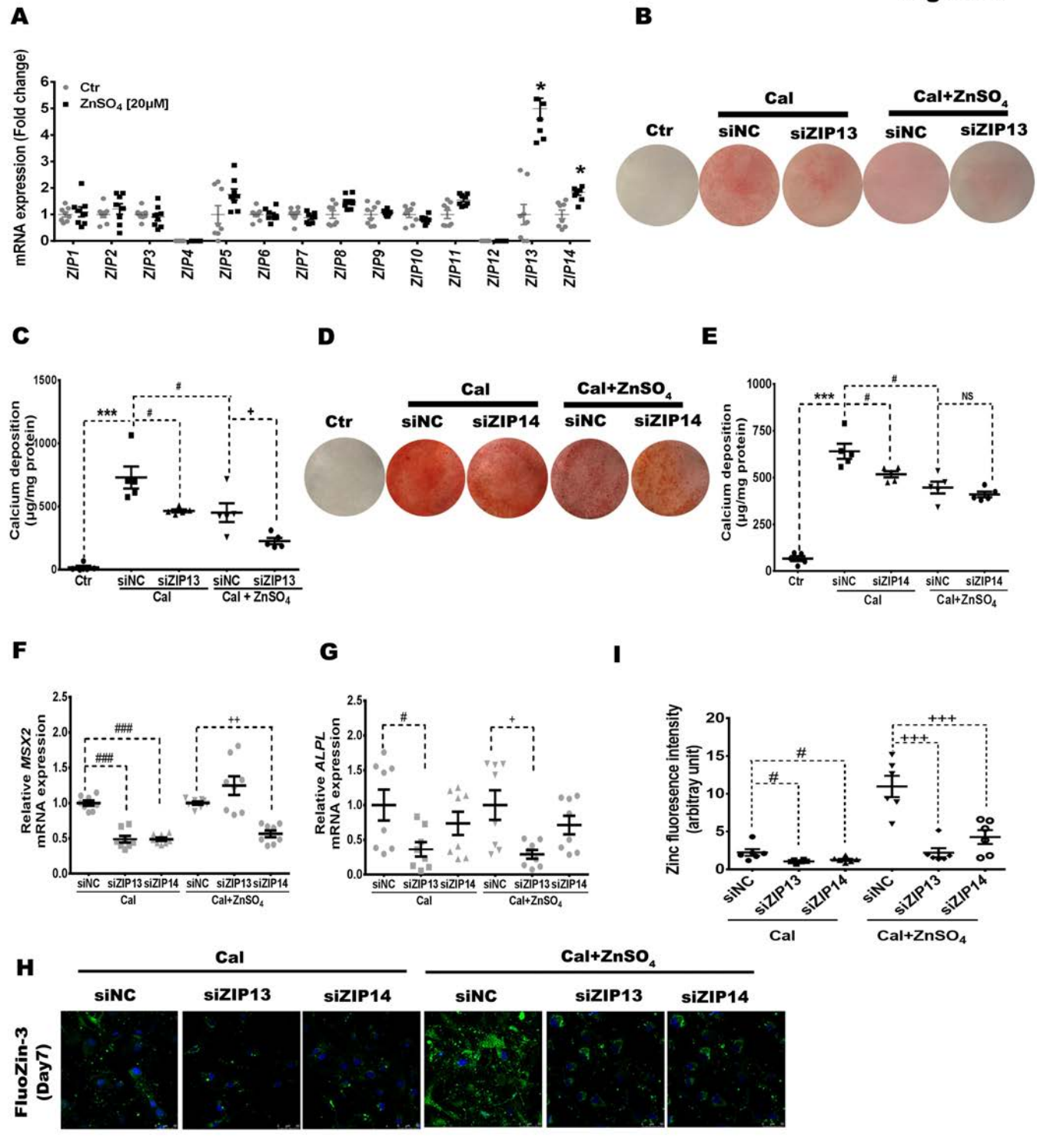
A
mRNA expression (Fold change)
Ctr
ZnSO4 [20μM]
ZIP1
ZIP2
ZIP3
ZIP4
ZIP5
ZIP6
ZIP7
ZIP8
ZIP9
ZIP10
ZIP11
ZIP12
ZIP13
ZIP14
B
Cal
Cal+ZnSO4
Ctr
siNC
siZIP13
siNC
siZIP13
C
Calcium deposition (μg/mg protein)
Ctr
siNC
siZIP13
siNC
siZIP13
Cal
Cal + ZnSO4
D
Cal
Cal+ZnSO4
Ctr
siNC
siZIP14
siNC
siZIP14
E
Calcium deposition (μg/mg protein)
NS
Ctr
siNC
siZIP14
siNC
siZIP14
Cal
Cal+ZnSO4
F
Relative MSX2 mRNA expression
siNC
siZIP13
siZIP14
siNC
siZIP13
siZIP14
Cal
Cal+ZnSO4
G
Relative ALPL mRNA expression
siNC
siZIP13
siZIP14
siNC
siZIP13
siZIP14
Cal
Cal+ZnSO4
I
Zinc fluoresence intensity (arbitray unit)
siNC
siZIP13
siZIP14
siNC
siZIP13
siZIP14
Cal
Cal+ZnSO4
H
Cal
Cal+ZnSO4
siNC
siZIP13
siZIP14
siNC
siZIP13
siZIP14
FluoZin-3 (Day7)

Figure 6

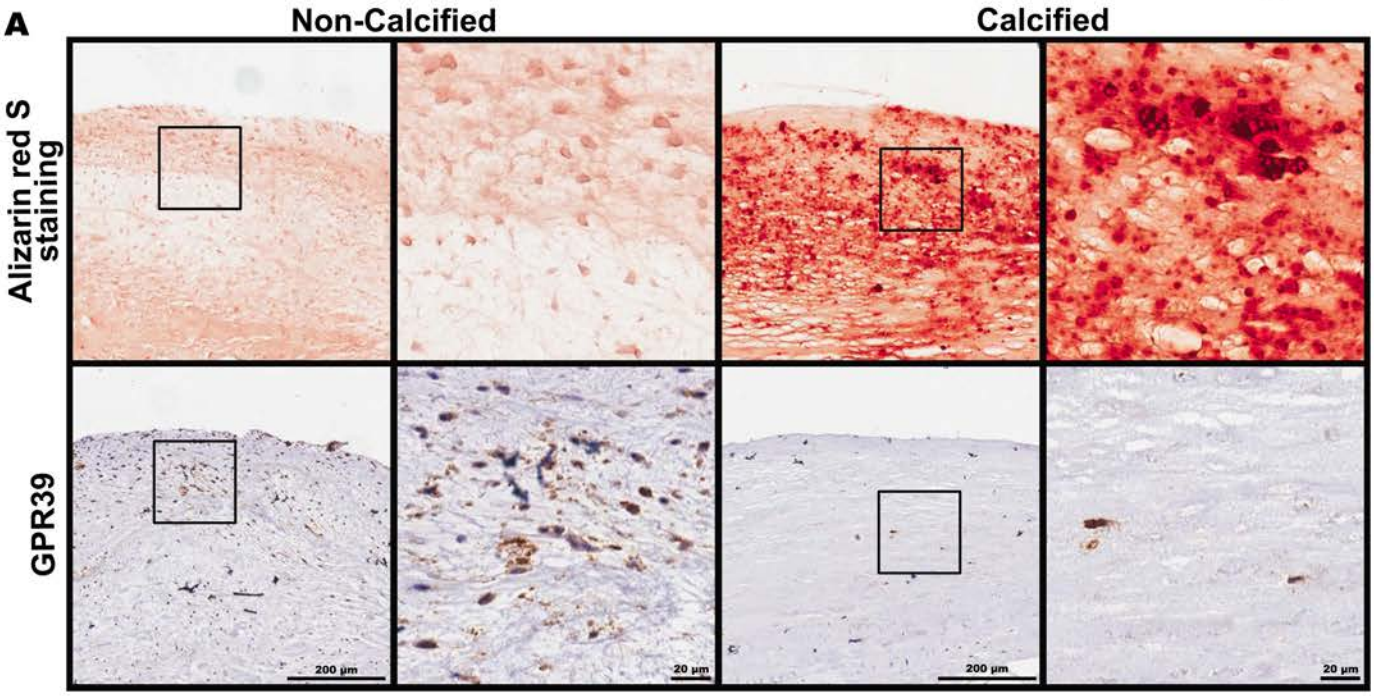
A
Non-Calcified
Calcified
Alizarin red S staining
GPR39
200 µm
20 µm
200 µm
20 µm

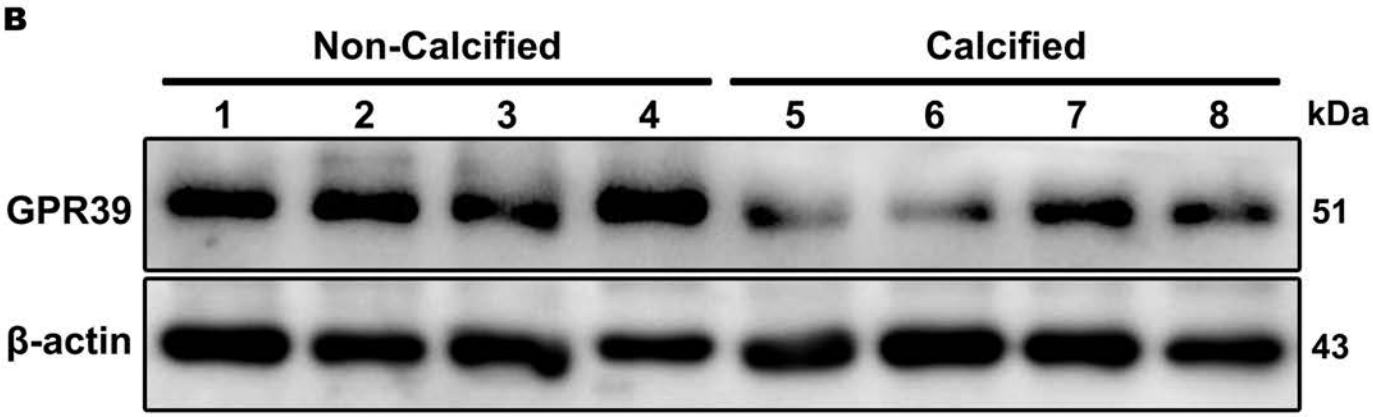
B
Non-Calcified
Calcified
1
2
3
4
5
6
7
8
kDa
GPR39
51
β-actin
43

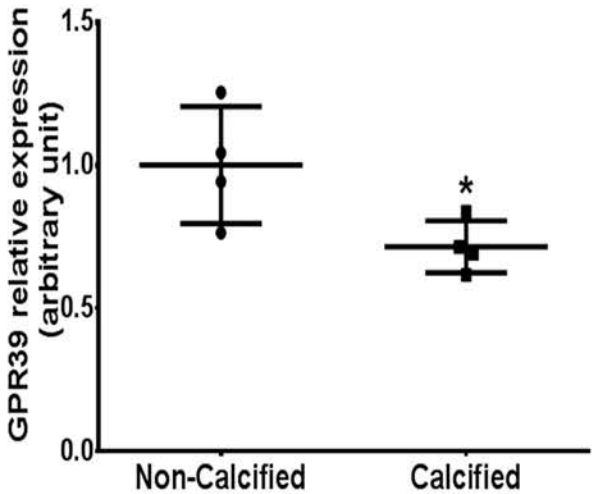
GPR39 relative expression (arbitrary unit)
1.5
1.0
0.5
0.0
*
Non-Calcified
Calcified

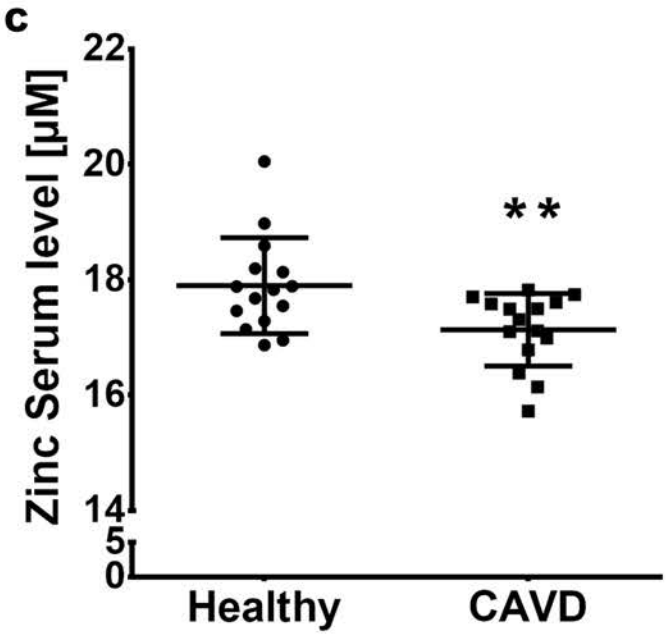
c
Zinc Serum level [µM]
22
20
18
16
14
5
0
**
Healthy
CAVD

Figure 7

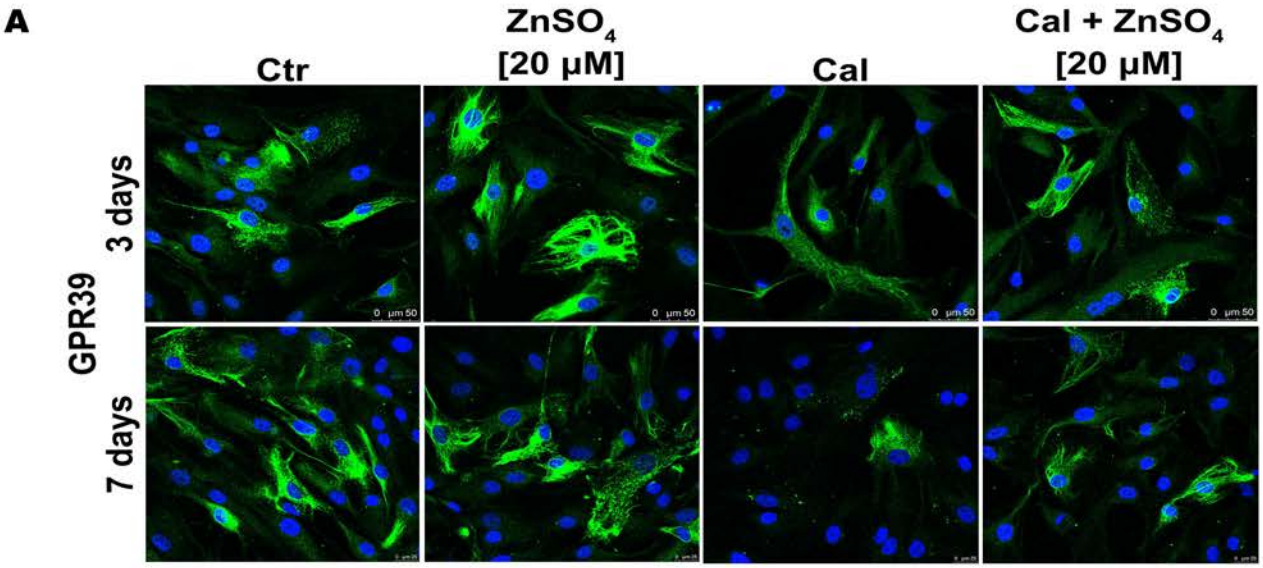
A
Ctr
ZnSO4 [20 μM]
Cal
Cal + ZnSO4 [20 μM]
GPR39
3 days
7 days

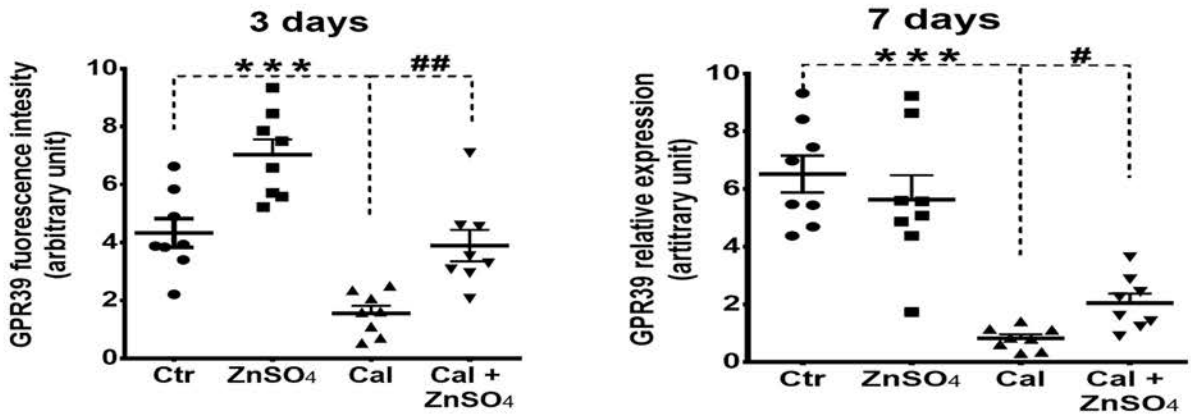
3 days
GPR39 fuorescence intesity (arbitrary unit)
***
##
Ctr
ZnSO4
Cal
Cal + ZnSO4
7 days
GPR39 relative expression (artitrary unit)
***
#

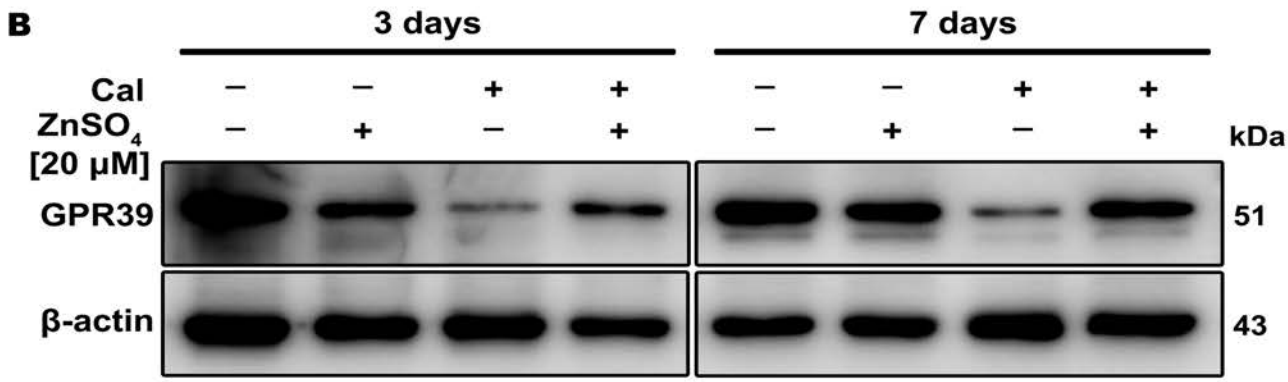
B
3 days
7 days
Cal
ZnSO4 [20 μM]
kDa
GPR39
51
β-actin
43

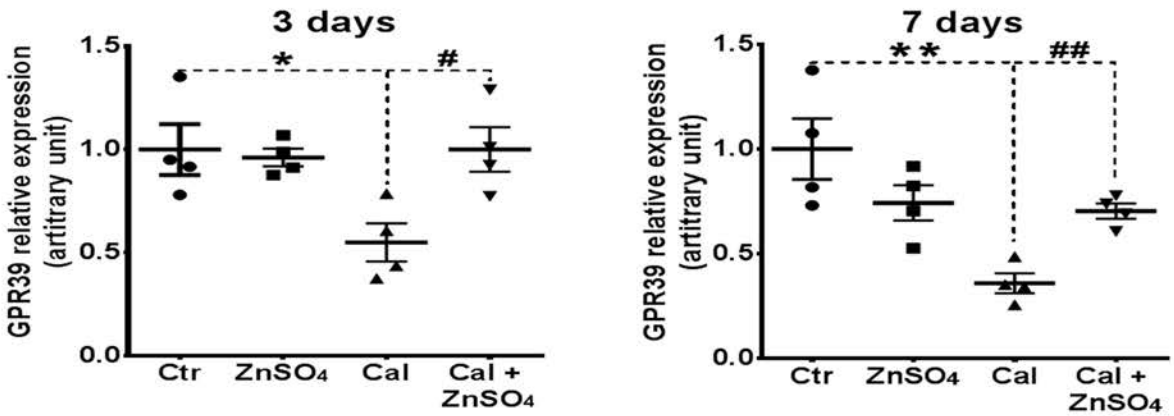
3 days
GPR39 relative expression (artitrary unit)
*
#
Ctr
ZnSO4
Cal
Cal + ZnSO4
7 days
**
##

Unedited western blot gels for Figure 2D

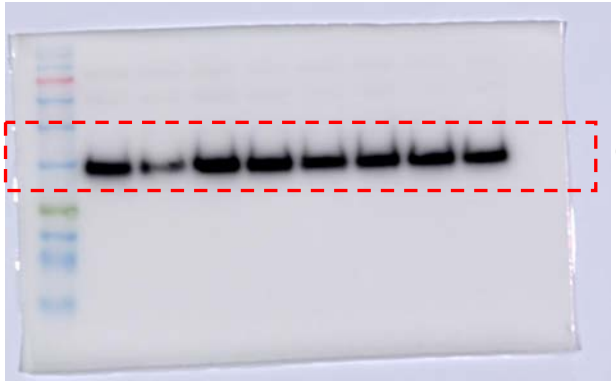

Caspase 3

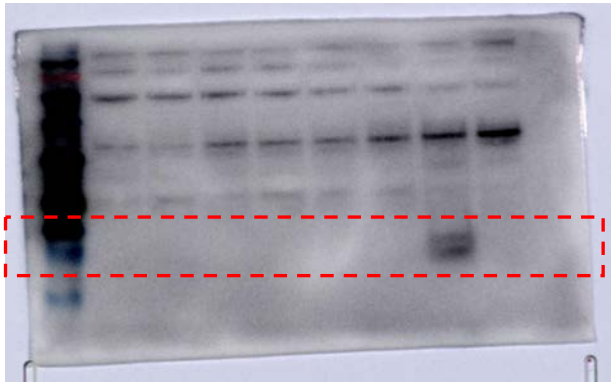

Cleaved Caspase 3

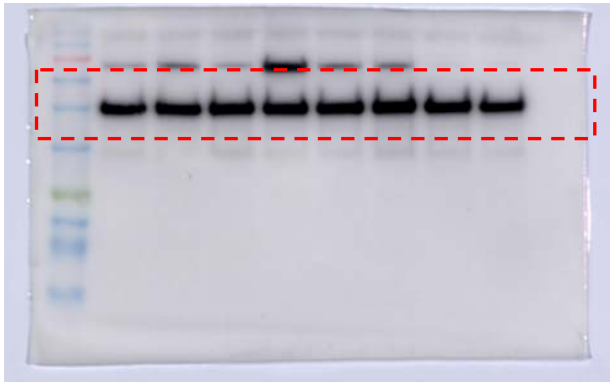

β-actin

Unedited western blot gels for Figure 3A

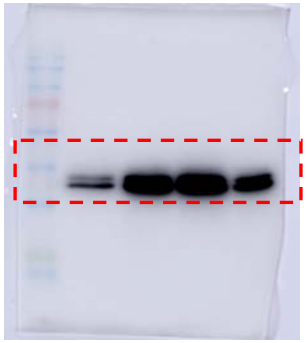

p-ERK

p-Akt

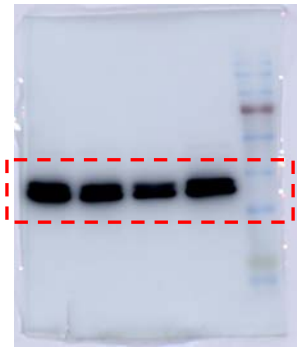

ERK

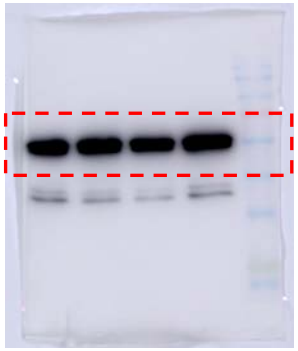

Akt

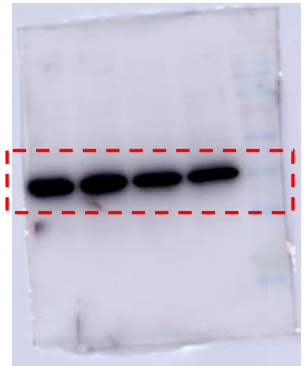

β-actin

Unedited western blot gels for Figure 3D

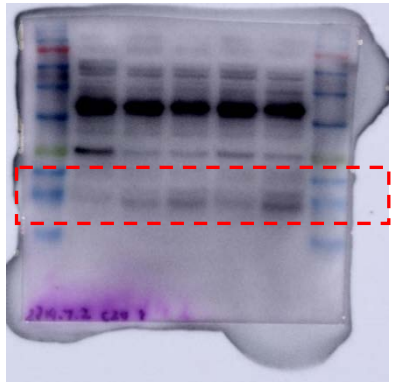

Cleaved Caspase 3

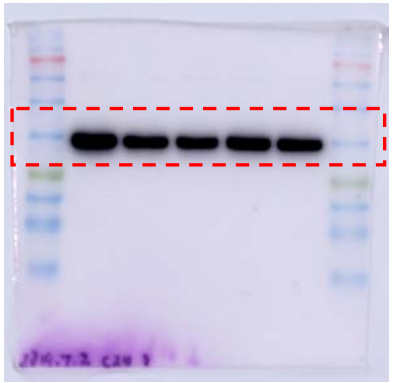

Caspase 3

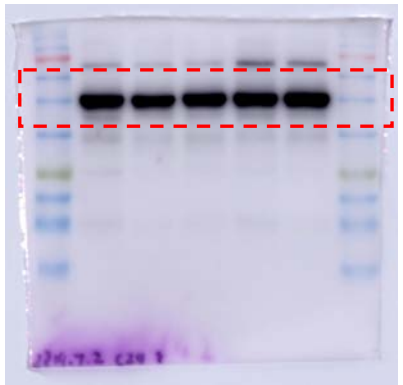

β-actin

Unedited western blot gels for Figure 4A

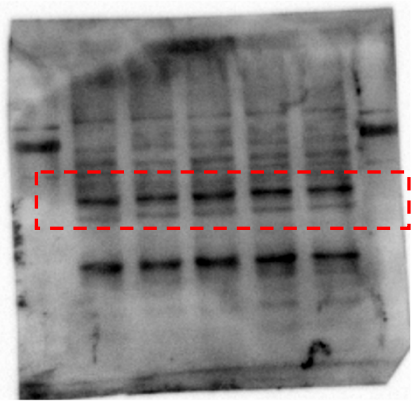

GPR39

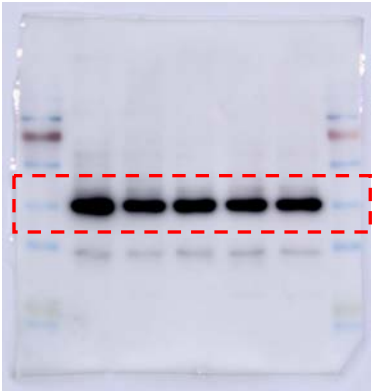

β-actin

Unedited western blot gels for Figure 4B

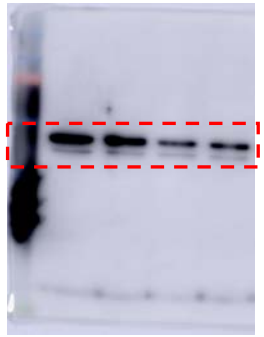

GPR39

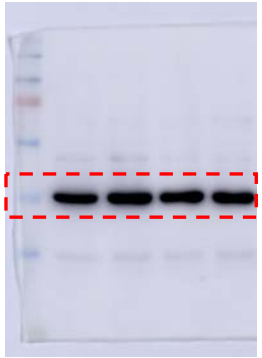

β-actin

Unedited western blot gels for Figure 4C

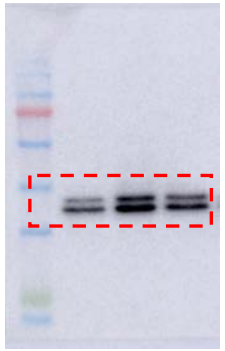

p-ERK

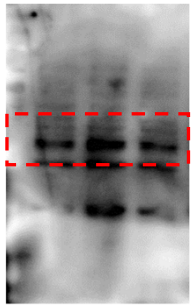

GPR39

ERK

β-actin

Unedited western blot gels for Figure 4F

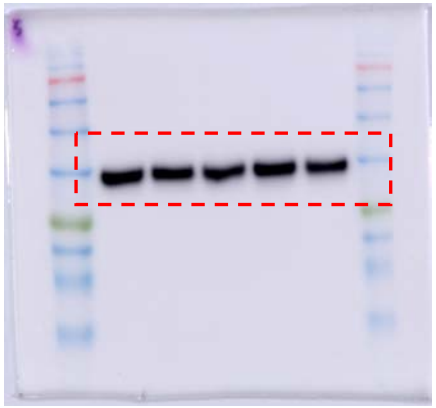

Caspase 3

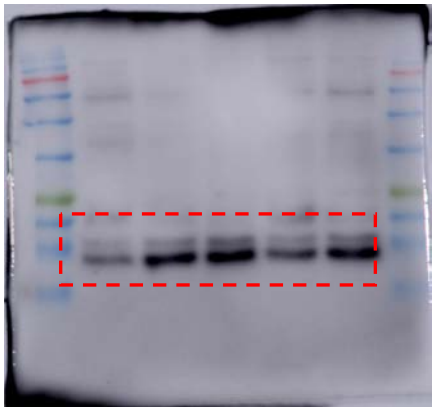

Cleaved Caspase 3

β-actin

Unedited western blot gels for Figure 6B

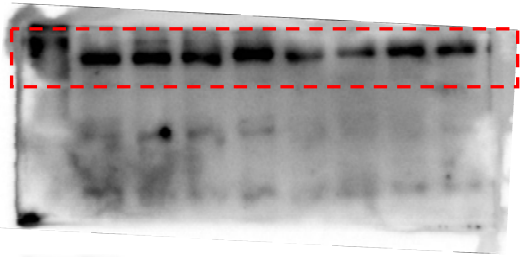

GPR39

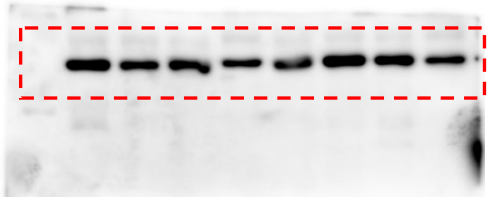

β-actin

Unedited western blot gels for Figure 7B

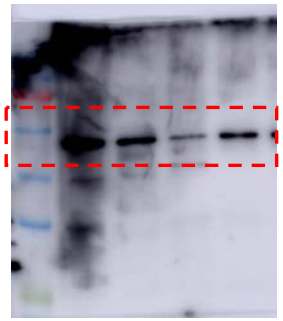

GPR39

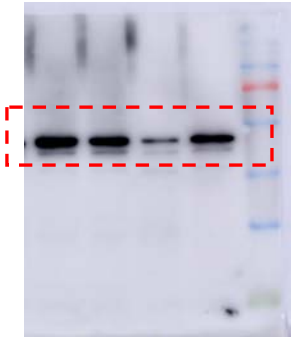

GPR39

β-actin

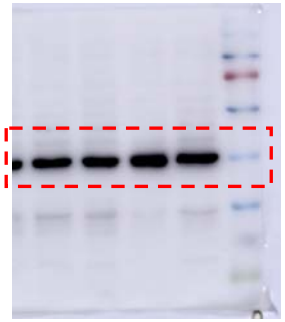

β-actin

Unedited western blot gels for Supplementary Figure V B

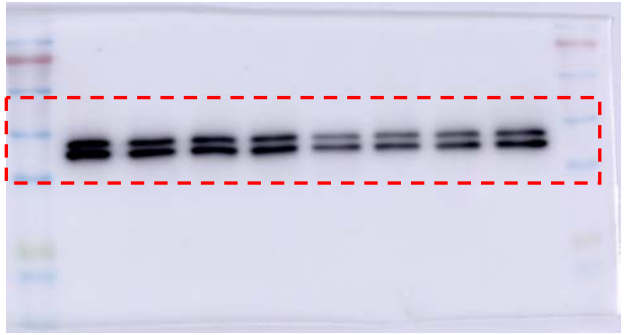

ERK

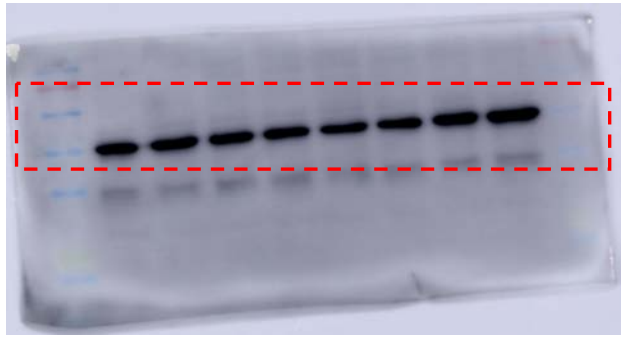

β-actin

Unedited western blot gels for Supplementary Figure V E

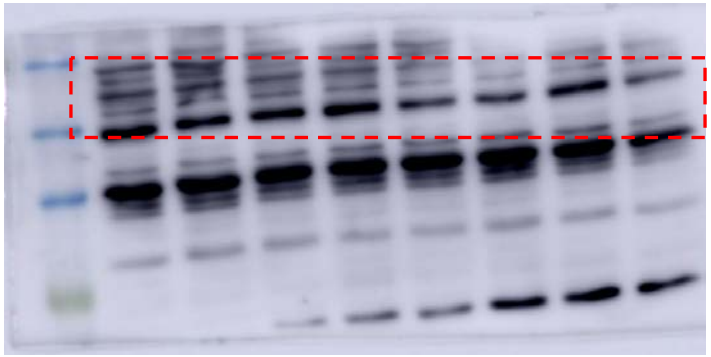

ZIP13

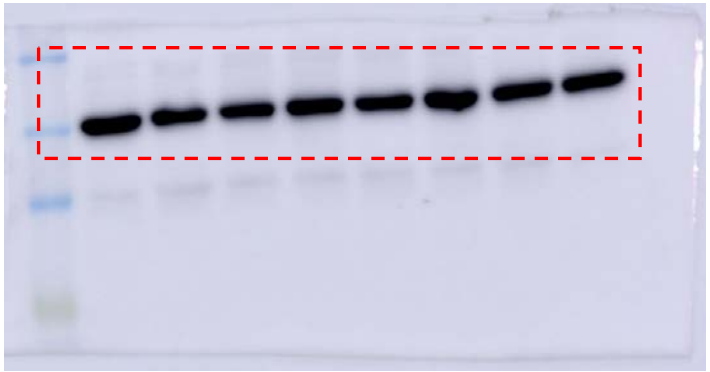

β-actin

Unedited western blot gels for Supplementary Figure V H

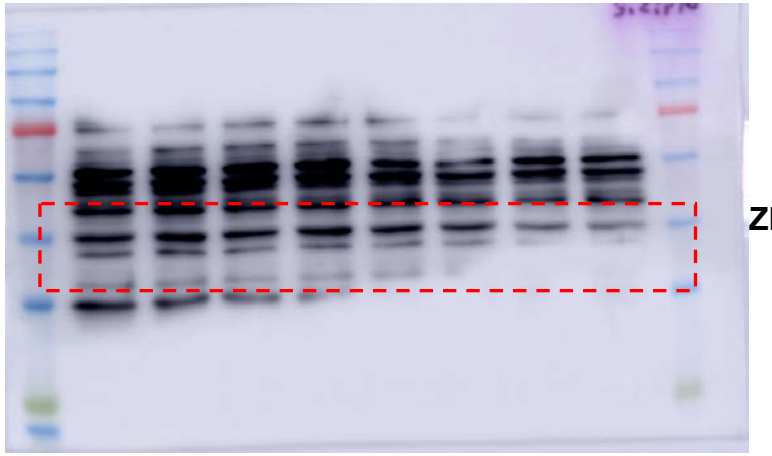

ZIP14

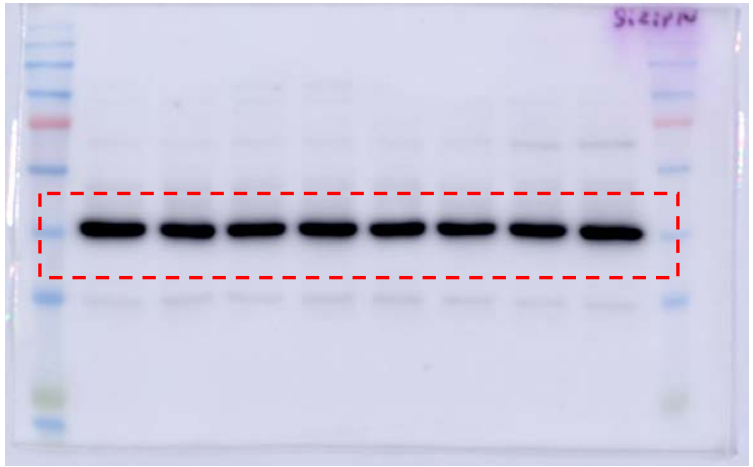

β-actin

Unedited western blot gels for Supplementary Figure VI A

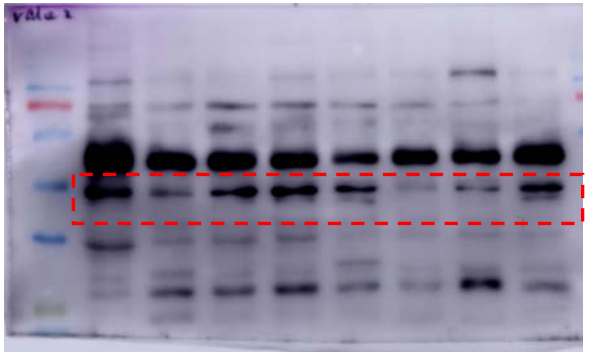

ZIP13

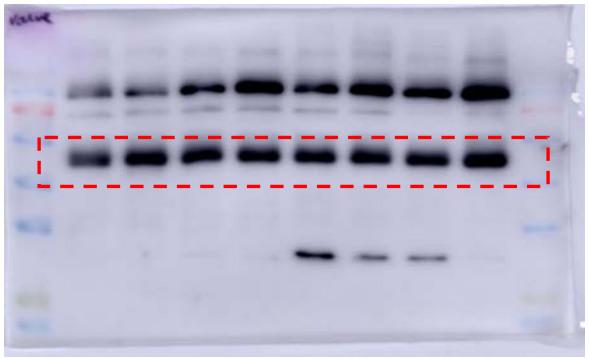

ZIP14

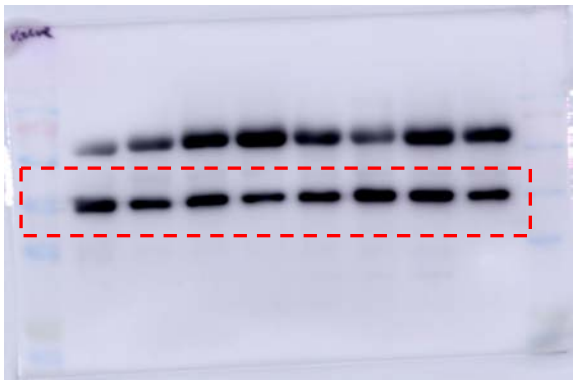

β-actin